Calhoun
Institutional Archive of the Naval Postgraduate School

Calhoun: The NPS Institutional Archive

DSpace Repository

Theses and Dissertations | 1. Thesis and Dissertation Collection, all items

1984

Measurement and analysis of spark ignition engine pressure data to determine heat release profiles.

Nelson, Fred Eldon

Massachusetts Institute of Technology

http://hdl.handle.net/10945/19439

Downloaded from NPS Archive: Calhoun

DUDLEY KNOX LIBRARY

http://www.nps.edu/library

Calhoun is the Naval Postgraduate School's public access digital repository for research materials and institutional publications created by the NPS community. Calhoun is named for Professor of Mathematics Guy K. Calhoun, NPS's first appointed -- and published -- scholarly author.

Dudley Knox Library / Naval Postgraduate School
411 Dyer Road / 1 University Circle
Monterey, California USA 93943

DEPARTMENT OF OCEAN ENGINEERING
MASSACHUSETTS INSTITUTE OF TECHNOLOGY
CAMBRIDGE, MASSACHUSETTS 02139

MEASUREMENT AND ANALYSIS OF SPARK IGNITION ENGINE PRESSURE DATA TO DETERMINE HEAT RELEASE PROFILES

by

Fred Eldon Nelson

SM (NAME)
SM (ME)

COURSE XIII-A
June 1984

Thesis
N36145

MEASUREMENT AND ANALYSIS

OF SPARK IGNITION ENGINE PRESSURE DATA

TO DETERMINE HEAT RELEASE PROFILES

by

© FRED ELDON NELSON

B.A., University of Minnesota
(1975)

Submitted to the Department of Ocean Engineering
in Partial Fulfillment of the
Requirements of the Degrees of

MASTER OF SCIENCE IN NAVAL ARCHITECTURE AND MARINE ENGINEERING

and

MASTER OF SCIENCE IN MECHANICAL ENGINEERING

at the

MASSACHUSETTS INSTITUTE OF TECHNOLOGY

May 1984

The author hereby grants to M.I.T. and the U.S.Government permission to reproduce and distribute copies of this thesis document in whole or in part.

TK5104
.U36145

MEASUREMENT AND ANALYSIS OF SPARK IGNITION ENGINE PRESSURE DATA TO DETERMINE HEAT RELEASE PROFILES

by

FRED ELDON NELSON

Submitted to the Department of Ocean Engineering
in partial fulfillment of the requirements of the degrees of
Master of Science in Naval Architecture and Marine Engineering
and Master of Science in Mechanical Engineering

ABSTRACT

Heat release analysis can be computed from the measured cylinder pressure at known cylinder volumes through the use of the First Law of Thermodynamics and the ideal gas law. After correcting for crevice effects and heat transfer to the combustion chamber walls, the combustion heat release profile can be determined. From the combustion heat release profile, the burn rate and the mass fraction burned can be calculated for studies of knock and turbulence.

The Ricardo Hydra MK III engine is instrumented, the operating properties are checked and the cylinder pressure is measured for fired and motored operating conditions at six different load and speed setpoints. The generated pressure data is then used in the Sloan Automotive Lab heat release model to determine the validity of the model for real engine data. The model is checked for scaling by load and speed. The heat release was successfully modeled using one set of model parameters for this engine operating at the different loads and speeds.

Thesis Advisor: John B. Heywood

Title: Professor of Mechanical Engineering

ACKNOWLEDGEMENTS

The author wishes to express his gratitude to Professor John B. Heywood for his guidance and technical assistance throughout this project.

Many thanks are also due the Sloan Automotive Laboratory Staff, Don Fitzgerald, Sal Albano, and Duane Page for their help with testing, equipment and the computer.

Sincere appreciation also goes to Chun Kwang-Min, for his assistance in the data collection, and to Eric Balles and Jan Gatowski for taking time to answer my many questions.

And sincerest appreciation to my wife, Alison, for typing this work.

TABLE OF CONTENTS

		PAGE
TITLE PAGE		1
ABSTRACT		2
ACKNOWLEDGEMENTS		3
TABLE OF CONTENTS		4
CHAPTER ONE:	INTRODUCTION	6
CHAPTER TWO:	THEORETICAL BACKGROUND	7
	1. First Law Analysis	
	2. Crevice Affect	
	3. Heat Transfer	
	4. Determination of γ	
	5. Residual Gas	
	6. Combustion Heat Release	
CHAPTER THREE:	ENGINE, INSTRUMENTATION, VERIFICATION, AND DATA ACQUISITION	17
	1. Engine and Dynamometer	
	2. Engine Instrumentation	
	3. Data Acquisition a. Equipment Hookup b. Procedure	
	4. Engine Setup Verification Procedures a. TDC b. Phasing c. η_v and Inlet Pressure d. Torque and MEP e. F/A Measurements and ϕ	

TABLE OF CONTENTS (CONT.)

		PAGE
CHAPTER FOUR:	ANALYSIS, RESULTS, DISCUSSION	29
	1. Computer Program	
	2. Calibration of the Model 4.2.1. Variation of the Model Parameters 4.2.2. Best Fit of the Model Parameters	
	3. Results	
	4. Discussion	
CHAPTER FIVE:	CONCLUSION	41
REFERENCES		43
APPENDIX A	ENGINE DATA SUMMARY SHEET	44
APPENDIX B	ENGINE SETUP AND VERIFICATION CHARTS	45
APPENDIX C	AFFECT OF VARYING MODEL PARAMETERS	59
APPENDIX D	BEST FIT HEAT RELEASE CURVES	66
APPENDIX E	CALCULATION FOR BEST FIT CURVES	79
APPENDIX F	COMPARISON OF LOADS AND SPEEDS	82
APPENDIX G	FUEL - AIR FLOW CALCULATIONS	88

CHAPTER ONE

INTRODUCTION

Many studies have been made using internal combustion engine pressure data to determine engine preformance. The thermal energy of the working fluids inside the engine can be accounted for through use of the cylinder pressure data. Heat release analysis can help determine the energy release during combustion and the energy loss from heat or mass transfer during an engine cycle. Few studies have been made to determine how well the heat release model will scale with engine load and engine speed. A study of this nature would assist in determining the validity of a heat release model.

Heat release analysis is computed from measured cylinder pressure at known cylinder volumes and through use of the First Law of Thermodynamics and the ideal gas law. This allows for determination of the apparent heat release inside the cylinder. By adding the effects of the heat transfer to the walls and the affects of the cylinder crevices, the heat release due to combustion can be determined. The value of the total heat released during combustion can be compared to the chemical energy introduced for that cycle to determine the validity of the model.

This work deals in three main areas. First, the engine setup, instrumentation and verification checks for the Ricardo HYDRA MK III engine from which the pressure data was taken and reviewed. Second, the data aquisition procedure is described. Third, the heat release analysis and results are discussed.

CHAPTER TWO

THEORETICAL BACKROUND

2.1 FIRST LAW ANALYSIS

Analysis of the cylinder contents of an internal combustion engine usually starts with the first law for an open system.

$$\delta U = \delta Q - \delta W + \Sigma m_i h_i$$

where U is the internal energy of the gases inside the cylinder, Q is the heat transfer across the boundaries, W is the work done by the system on the control volume and $m_i h_i$ is the energy flow due to mass flow across the system boundary.

For the internal combustion engine system, U represents the sensible internal energy which is a function of temperature and can be written as:

$$U = mc_v T$$

where m is the mass in the cylinder, c_v is the constant volume specific heat and T is the average cylinder temperature. Using the ideal gas law pV = mRT, U can be rewritten as:

$$U = \frac{c_v pV}{R}$$

The piston work, δW, can be written as pdV.

The heat transfer Q can be divided into two parts:

Q_c, the heat addition due to combustion and

Q_w, the heat transfer to the combustion chamber walls.

Using the additional relations: $c_p - c_v = R$, $\gamma = c_p/c_v$, $h = c_p T$ and rearranging, the first law equation becomes:

$$\delta Q_c = \delta Q_w + \frac{\gamma}{\gamma-1} Vdp + \frac{1}{\gamma-1} Vdp + c_p Tdm$$

Considering a closed system (figure 2-1) from intake valve closing to exhaust valve opening, eliminates the changing mass term. The first law equation becomes:

$$\delta Q_c = \delta Q_w + \frac{\gamma}{\gamma-1} Vdp + \frac{1}{\gamma-1} Vdp$$

The net heat release, equal to the heat added by combustion minus the heat transferred to the walls, can be calculated from the measured pressures, the known cylinder volume, and the known rate of change of the cylinder volume.

2.2 CREVICE AFFECT

For the first law derivation of the heat release equation, the system was considered to be a closed system and the changing mass term was dropped. However, there are spaces with low volume to surface area ratios where the wall temperature has a greater efect. Usually called crevices, these spaces include gaps for the head gasket, for the spark plug threads, and the volume between the piston and the cylinder wall down to the piston rings (which is typically the largest crevice volume). These regions can be grouped together and modeled as a single crevice control volume (figure 2-1). The crevice volume is typically 1 to 2% of the clearance volume, but due to the cooling effect of the large surface area, the crevice may contain 6-10% of the cylinder mass.

The temperature of the mixture in the crevice can be modeled as equal to the temperature of the cylinder gases for mass flow into the crevice but equal

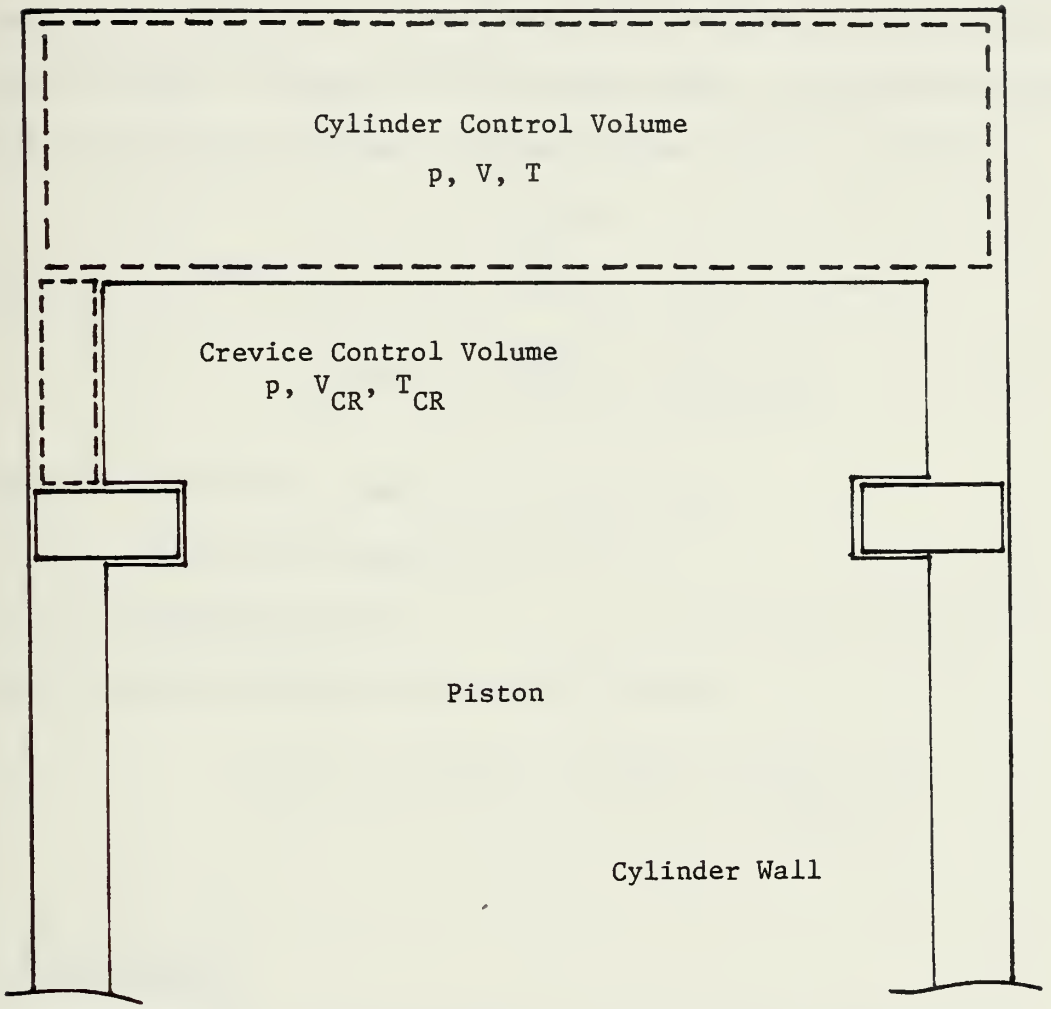

Figure 2-1. Cylinder and Crevice Control Volumes

to the wall temperature for mass flow out of the crevice. This difference in temperature of the mass flow represents a loss of energy from the cylinder control volume. To account for this energy change, the mass effect term for the crevice must be included in the heat release equation. This term:

$$c_p T dm$$

can also be changed by using the relation pV = mRT as follows:

$$c_p T(dm) = c_p T \left[\frac{V dp_{cr}}{RT_{cr}}\right] = \frac{\gamma}{\gamma-1} \frac{T^*}{T_{cr}} V_{cr} dp$$

where T^* = crevice wall temperature for $d_m \geq 0$ and

T^* = cylinder gas temperature for $d_m < 0$

cr = indicates crevice

With this term, the heat release equation becomes:

$$\delta Q_c = \delta Q_w + \frac{\gamma}{\gamma-1} pdV + \frac{1}{\gamma-1} Vdp + \frac{\gamma}{\gamma-1} \frac{T^*}{T_{cr}} V_{cr} dp$$

2.3 HEAT TRANSFER

An estimate for the heat transfer to the walls must be made if the combustion heat release is to be separated from the net heat release. In general, heat transfer from a hot gas to the cool combustion chamber surface is written as:

$$Q = hA\Delta T$$

where h is the heat transfer coefficient, A is the combustion chamber surface area and ΔT is the temperature difference between cylinder gas and the cylinder wall. Woschni (1) developed an experimental correlation for heat transfer based on the Nusselt-Reynolds relationship:

$$N_u = \frac{hL}{k} = 0.035\ Re^{0.8}$$

The characteristic length used is the bore while the characteristic velocity in the Reynolds Number, Re, is proportional to the mean piston speed with a factor added for the combustion expansion velocity. This factor is used during the combustion and expansion phases of the engine cycle.

Woschni's correlation for the heat transfer coefficient is:

$$h(w/m^2k) = c_1 B(m)^{-0.2}\ p(atm)^{0.8}\ T(K)^{-0.53}\ W(m/s)^{0.8}$$

For this equation, c_1 is a constant, B is the cylinder bore, p and T are the average cylinder pressure and temperature and W is the characteristic velocity. The value for the characteristic velocity is calculated from:

$$W\left[\frac{m}{s}\right] = 2.28\ \bar{S}_p\left[\frac{m}{s}\right] + c_2\left[\frac{V_D}{V_i}\right]\left[\frac{p_f - p_m}{p_i}\right] T_i(K)$$

where $\bar{S}_p$ is the mean piston speed, c_2 is a constant, V_D is the cylinder volume, P_f and P_m are the fired and the motored pressures for that position, and V_i, P_i, and T_i are the cylinder conditions at the intake valve closing. Woschni empirically found c_1 to equal 110 and c_2 to equal 3.24×10^{-3}. To achieve consistancy with S.I. units, the value for c_1 was changed to 3.26 in the computer program.

For the engine anaylsis, the computer program used to calculate the heat release was written to multiply Woschni's c_1 (=3.26) and c_2 ($=3.24 \times 10^{-3}$) by an input value of C_1 and C_2. The input value of C_1 and C_2 are the variables that scale the heat release model to the Ricardo engine data.

Woschni's heat transfer correlation can also be modified by changing the exponents which scales the heat transfer coefficient with engine speed. Woschni's formula can be written as:

$$h = c_1 B^{(1-n)} p^n T^{(0.75-1.62n)} W^n \qquad (1)$$

where n is the exponent. With n = 0.8, the original equation is recovered.

2.4 DETERMINATION OF GAMMA (γ)

γ ($=c_p/c_v$) is an important parameter in the heat release model. It is a parameter which varies as a function of both pressure and temperature, and with the proportions of unburned and burned gases. To use γ in the heat release model, it is convenient to regard γ as a simple function of temperature, in this case, a linear function of temperature.

To obtain γ as a function of temperature, cylinder pressure and temperature were calculated from the experimental data at various points and plotted on the chart of γ versus temperature as given in Mansouri and Heywood(2). A calculation of γ for the unburned mixture was made for the temperature from $500^{o}K$ to $1500^{o}K$. These points were also plotted and a least squares linear curve fit was drawn through both sets of points (figure 2-2). The equation for this line was incorporated into the heat release model.

The mass in the cylinder was required in order to calculate the temperature in the cylinder using the ideal gas law. The mass in the cylinder:

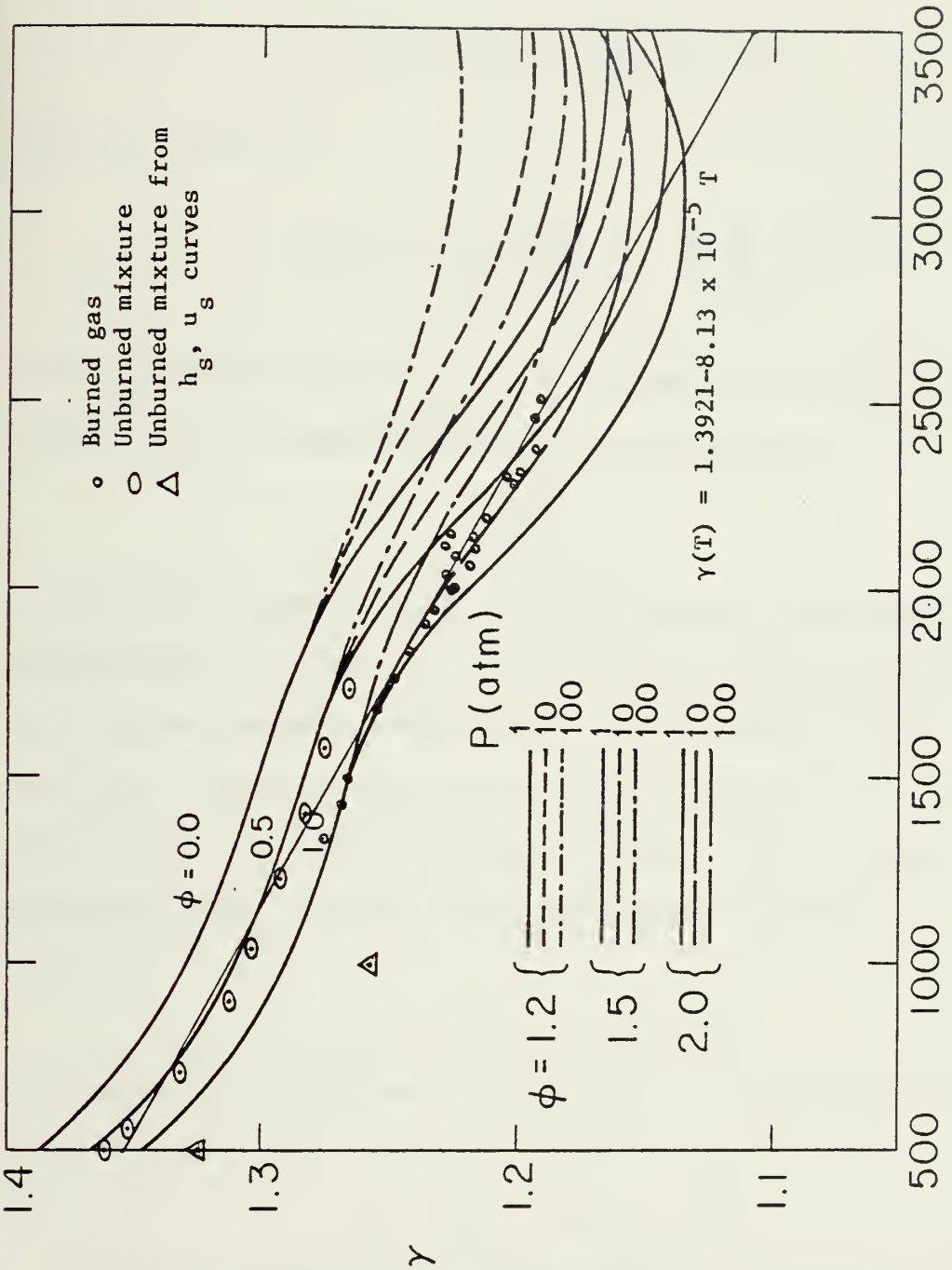

Figure 2-2. γ vs. T for Indolene at ϕ = 1.0

$$\text{mass} = m_a + m_f + \frac{X_R}{1-X_R}\left[m_a + m_f\right]$$

can be written as:

$$m\left[\frac{g}{cyc}\right] = \frac{1}{1-X_R}\left[\frac{\dot{m}_a\left[\frac{g}{s}\right]120}{RPM} + \frac{\dot{m}_f\left[\frac{g}{s}\right]120}{RPM}\right]$$

where X_R is the residual fraction, m_a is the mass of air, and m_f is the mass of fuel. Using the measured pressure and the known volume:

$$T = \frac{P \times VOL}{m \times R}$$

The plotted values for γ unburned were calculated using a mass-fraction weighted sum of γ air and γ fuel at $\phi = 1.0$. γ fuel was determined by interpolating Indolene's average molecular weight between the value of C_6H_{14} and C_8H_{18}. The mass weighted value of γ for the fuel air mixture was subtracted for γ air and the difference was plotted on the γ versus temperature chart. The result of the least squares curve fit for the data points is:

$$\gamma(T) = 1.3921 - 8.13 \times 10^{-5}\ T$$

This varies little from a previous equation for γ of propane and air at $\phi = 0.9$ which is:

$$\gamma(T) = 1.3751 - 6.9910 \times 10^{-5}\ T$$

Two points were checked for the unburned mixture at 500°K and 1000°K for isooctane at $\phi = 1.0$. These values of γ were calculated by finding the slope of h_s and u_s at 500°K and 1000°K from using reference 3 and using the relationships:

$$c_p = \frac{dh}{dT} \qquad c_v = \frac{du}{dT} \qquad \gamma = \frac{c_p}{c_v}$$

These two points are also shown in figure 2-2.

2.5 RESIDUAL GAS

Residual gas, the exhaust gas remaining in the cylinder after intake is completed, affects the amount of the new fuel and air that can be drawn into the cylinder and therefore affects the energy entering the system. Residual gas fractions were calculated from the graphs of Toda, et al (4). Engine A was chosen for its valve timing and because it has 27° of valve overlap close to the 24° for the Ricardo engine. The compression ratio of 8.5 was chosen compared to 8.41 for the Ricardo engine. The residual gas fraction changes little with the changing air fuel ratio so 14.5 was used versus 14.37. The final graph was entered using the intake pressure and the value of the residual gas was obtained by interpolating for the speed. The values for residual gas are listed on the engine data sheets (Appendix A).

2.6 COMBUSTION HEAT RELEASE

The net heat release is obtained by considering the cylinder as a closed system, modifing for the mass loss to the crevice, and by considering the combination of chemical energy added and the heat transfer to the walls as a "net heat addition". By separating the heat transfer to the wall from the "net heat addition", the combustion heat release is obtained:

$$\delta Q_c = \delta Q_w + \frac{\gamma}{\gamma-1} pdV + \frac{1}{\gamma-1} Vdp + \frac{\gamma}{\gamma-1} \frac{T^*}{T_{cr}} V_{cr} dp$$

The total combustion heat release obtained can be compared with the fuel energy added to determine the validity of the model. The best choice of parameters can be calculated by finding the error for each of the engine data points and model conditions. The error is found by the following equation:

$$m_f(LHV)\eta_{comb} - (Q_{gross})_{max} = e$$

The best fit is the model condition for which the square root of the sum of the errors squared is the smallest.

$$\text{Best fit} = \text{MIN } (\Sigma e^2)^{0.5}$$

The model parameters varied are C_1, C_2, and n in Woschni's correlation, and the crevice volume and the wall temperature in the heat release analysis.

CHAPTER THREE

ENGINE, INTRUMENTATION, DATA COLLECTION AND PERFORMANCE VERIFICATION

3.1 ENGINE AND DYNAMOMETER

The engine used for data collection is a Ricardo HYRDA MK III (5) single-cylinder spark-ignition engine (figures B-1 and B-2). It is designed as a high speed research engine typical of the engines used in today's cars. Its compression ratio is 8.41, its displaced volume is 496 cm^3 and it has a bore and stroke of 8.57 cm and 8.6 cm respectively. The engine has Bosch timed electronic-fuel- injection with a separate electronic fuel pump. The fuel used is Indolene, a standard reference gasoline. Indolene characteristics (figure B-4) include a research octane number of 97.2 and it is therefore resistant to knock. The engine operating range is from 1000 RPM to 5400 RPM. It has a maximum power output of 15 kW.

The engine is directly coupled to an EATON Dynamometer 6000 series adjustable-frequency regenerative dynamometer of 100 HP capacity. It has a strain gage which is calibrated by the dead weight method to give a direct readout of torque in foot pounds (lb_f-ft). The dynamometer can operate in speed control mode which maintains a set speed while allowing the load to vary, or it can operate in load control while letting the speed vary. In the speed control mode, the dynamometer can provide drive force only, absorb only, or both drive and absorb when in universal mode. Similarly, the load control can provide either a drive or an absorb load.

3.2 ENGINE INSTUMENTATION

The pressure transducer used to measure cylinder pressure is a Kistler 7061 piezoelectric pressure transducer mounted in the cylinder head coupled to a Kistler charge amplifier. The coupled set was calibrated by the dead weight method as per Lancaster, et al (6). The equation of the line as calibrated for 20 points from 0 to 1000 psi is millivolts = 1.7 + 4.985 x pressure (psi) with R^2 = 1.0000 (figure B-5).

Engine temperature measurements were made through use of type K chromel alumel thermocouples. Thermocouples were installed to measure the oil temperature, the water inlet and the water outlet temperatures from the head and cylinder. The air inlet and the exhaust temperatures were also measured along with the temperature of the fuel from the buret.

Three manometers for pressure measurements were installed. These were:

(1) a mercury manometer to measure the time-average intake pressure just downstream of the throttle,

(2) a water manometer to measure the air flow laminar-flow-element pressure drop (which is upstream of the throttle), and

(3) a water manometer to measure the average exhaust pressure.

The air flow is measured by an Alcock viscous flow air meter which measures the differential pressure across a laminar flow element. This pressure difference is measured with a special manometer that allows variations in the air flow ranges. The factory calibration showed better than 3% linearity. The measured air flow in m^3/sec is converted to gm/sec at NTP to obtain the measured air mass flow rate.

The fuel system has a separate 12 V fuel pump with a pressure regulating return valve which maintains approximately 2 bar pressure at the fuel injection valve (figure B-6). The system is set up to draw and return fuel to the fuel tank during normal operations and while filling the buret. To measure fuel flow, the supply and return valves are simultaneously switched from the fuel tanks to the burets. The selection the large or small buret is made by the position of the buret petcocks. The flow out of the buret is measured in milliliters. The flow is timed and is then converted to a mass flow rate by dividing by the density of the fuel at the measured temperature (figure B-4 and Appendix G).

A shaft encoder is connected to the end of the engine crankshaft to provide 360 pulses per revolution plus one larger pulse per revolution. The single pulse per revolution is set at BDC to act as a trigger and as a reference point for the data aquistion system.

3.3 DATA ACQUISTION

A. Equipment hookup. The shaft encoder and charge amplifier are easily connected to the digitizer. The shaft encoder output goes to the tachometer interpreter board where the signal is separated into two outputs, a pulse per revolution output used as a trigger and a crank angle degree output. The pulse per revolution output goes through an amplifier to three places: the ocilloscope trigger, to the digitizer stop trigger and to channel 2 of the digitizer. The crank angle degree output is connected to the digitizer external clock. The pressure transducer output is connected to channel 1 of the ocilloscope and to channel 1 of the digitizer.

The connection of the computor terminal and the digitizer to the main computer system is accomplished by the Sloan Lab staff.

B. Data Acquisition procedures. After completing startup checks, the engine is motored and the throttle is set to the desired load. From the measured air flow, the approximate fuel setting is determined. Note, the air flow drops about 10 % between motoring and firing. The engine is then fired and the fuel and air flow measurements are taken. The fuel is adjusted until the equivalence ratio is about 1.0. The ϕ (exhaust) is calculated from the measurements taken from the exhaust gas cart analysis and compared to ϕ (intake) as measured. When these values confirm that $\phi \approx 1.0$, maximum brake timing (MBT) is then searched for. MBT can be found by adjusting the timing to obtain the maximum measured brake torque. An alternative method for determining MBT is from the calculated IMEP from $\int pdV$. After finding MBT (figure B-13), ϕ is checked to ensure that it is still equal to 1.0.

The actual data acquisition is straight forward. The digitizer parameters must be verified and then the digitizer is brought on line by the computor terminal, the stop trigger is disconnected and data collection proceeds. The stop trigger is reconnected and the acquired data is transfered to the VAX disc. The procedure is repeated for the number of sets of data required. The system records 44 cycles of data each time and normally two sets of 44 fired cycles were collected.

To collect motored data, the fuel injection is turned off just prior to the start of collection so that the engine has little time to cool off. After recording the motored data, the fuel injection is turned back on. The ϕ

(intake) versus the ϕ (exhaust) is checked and pictures of the pressure versus time on the oscilloscope are taken. Environmental conditions and motored conditions are checked and recorded and then the engine is changed to another setpoint.

3.4 ENGINE SETUP VERIFICATION PROCEDURES

a. TDC Location. The most important item on the engine requiring verification is the top dead center (TDC) marking. The position of TDC is checked by three different methods. The simplest method is to locate the piston at the marked TDC and rotate the engine in one degree increments about TDC to $\pm 5^{\circ}$. The dial indicator reading is noted at each degree.

The second and third methods are related. In the second method, the engine is rotated through bottom center (BC) to $\pm 60^{\circ}$ from TDC. A depth reading to the piston crown is taken, then the engine is rotated through BC to 61°, 60°, and 59° from TDC. A depth reading is taken at each of these positions and is compared to the first reading at $\pm 60^{\circ}$.

For the third check, an adaptor was made for the spark plug hole into which a sliding rod could be placed. The adaptor ensured that the rod is held vertical and touches the piston crown at the same spot during the entire check. A dial indicator is fastened to this rod and set to about half its full scale reading with the engine again positioned at $\pm 60^{\circ}$ from TDC. The engine is rotated through BC until the same reading is obtained on the dial indicator on the opposite side of TDC. All three checks were in agreement and indicated that the actual TDC was approximately 0.1° after the marked TDC.

This is well within the required accuracy of the data aquisition system and the heat release program.

b. Phasing. The next item requiring verification is the timing of the BC pulse from the shaft encoder. To verify this timing, the pulse output is connected to a strobetach. The engine is motored and the BC pulse is checked against the flywheel crankangle markings.

For additional checks of the phasing, motoring pressure data is taken. From this data, the average peak pressure location is determined. The peak pressure location for 1200 RPM at WOT is 1.00 $\pm$ 0.61 degrees before TDC. The log P-log V diagrams also were plotted from this information and the slopes checked for curvature according to Lancaster, et al (6). The phasing appears correct from the above checks (figure B-7 and B-8).

Another verification is to check peak pressure versus PV^N = constant. At 1200 RPM WOT, the transducer peak pressure is 1.2 V on the oscilloscope which equals 240 psig. 240 psig + 15 psi = 255 psia. With γ = 1.35, PV^N yields a value for P_2 = 260 psia. These results are very close.

c. η_v and inlet pressure. The volumetric efficiency η_v has also checked. Using ρ_{ao} of the air in the engine cell, η_v at 2500 WOT is 80 % for firing. The volumetric efficiency for motoring is typically 10 % higher due to 10 % higher air flow during motoring.

Prior to taking data, the data acquisition system requires a correction for bias and scaling. The scaling converts the charge amplifier input though the digitizer into a value of BITS/VOLT for use in the data acquisition system. The system is scaled as follows:

$$\frac{4.985 \text{ m V}}{\text{psi}} \times \frac{14.69595 \text{ psi}}{\text{atm}} \times \frac{4096 \text{ bits}}{10 \text{ Volts}} = 30.007 \frac{\text{bits}}{\text{atm}}$$

The data acquistion requires a negative scaling factor in atm/bits. So the scaling factor is:

$$- 3.33255 \times 10^{-2} \frac{\text{atm}}{\text{bits}}$$

The bias is set so that 4096 bits equals zero atmospheric pressure (zero Volts output from the charge amplifier). The full scale range of the data acquisition system is:

$$4096 \text{ bits} \times 3.33255 \times 10^{-2} \frac{\text{atm}}{\text{bits}} = 136.5014 \text{ atm}$$

Therefore the bias is set at 136.5 atm. Figure B-8 shows a log P-log V diagram drawn prior to setting the scale and bias. The curved compression and expansion lines indicate that an incorrect intake pressure was used for this graph. Figure shows the same data plotted after correcting for scale and bias.

The intake pressure measured on the intake manometer is not the actual pressure during the engine intake process. It is the average pressure in the intake port which equals P_I from about 12^o before TDC to 56^o after BC (i.e. 248^o of 720^o) and approximately equals atmospheric pressure the rest of the cycle. The initial approximation for P_I is made using the assumption that the air flow is proportional to the pressure. P_I is approximately as follows:

$$P_I(\text{During intake}) = P_{I(WOT)} \times \frac{\dot{m}_a}{\dot{m}_{a(WOT)}}$$

Using this value for P_I, the log P-log V diagrams for the fired data are graphed with P_I varied by 5 % increments of its estimated value. The slopes of the compression and expansion slope are checked for curvature and the intake and expansion lines are checked to ensure that the pressure in the cylinder is less than P_{atm} during intake and greater than P_{atm} during exhaust as per Lancaster, et al (6). The values that provide the best fit log P-log V diagrams are the values used for P_I in the heat release analysis.

d. Torque and MEP. Verification of the engine performance can be made by comparing the torque readout from the dynamometer with the engine IMEP. Defining the terms $IMEP_{gross}$ as the IMEP calculated from the pressure data for the compression and expansion strokes and $IMEP_{net}$ as the calculated IMEP for the entire engine cycle, the difference, $IMEP_{gross} - IMEP_{net}$, equals the pumping MEP or PMEP. The $IMEP_{gross}$ calculated from the $\int pdV$ can be compared to the $IMEP_{gross}$ calculated from the sum of the brake torque, the friction, and the pumping MEP. These $IMEP_{gross}$ values, when plotted against each other should result in a straight line with a slope of 1 (figure B-9). The $IMEP_{gross}$ from the $\int pdV$ is calculated by integrating the measured pressure over the known volume change. The IMEP (from torque) is calculated by the following method:

Brake MEP (from motored torque) = Rubbing friction MEP + PMEP (motored)

Therefore:

Rubbing friction MEP = Brake MEP (motored torque) - PMEP (motored)

$IMEP_{gross}$ (from torque) = Rubbing friction MEP + Brake MEP (from fired torque) + PMEP (fired)

The result of the calculation is that the IMEP (torque) is less than the IMEP($\int pdV$) at lower values of IMEP, but are approximately equal at higher values of IMEP.

$IMEP_{gross}$ calculated from pdV and the BMEP calculated from the torque can be plotted against the air flow normalized by the WOT air flow ($\dot{m}_a/\dot{m}_{aWOT}$). The linear least squares curve fit for $IMEP_{gross}$ is:

$$IMEP_{gross} = -4.71 + 152.8 \left[\frac{\dot{m}_a}{\dot{m}_{a\ WOT}} \right]$$

and for the BMEP from the measured torque is:

$$BMEP\ (torque) = -27.19 + 144.79 \left[\frac{\dot{m}_a}{\dot{m}_{a\ WOT}} \right]$$

The slopes of the plots of $IMEP_{gross}$ and BMEP (torque) from the least squares fit are nearly equal (152.8 versus 144.79). These results indicate that the calculated IMEP from the pressure data and the IMEP from the torque are compatible and that the motoring IMEP (friction and pumping) is approximately constant over the engine load and speed set points only increasing slightly (from 25 to 30 psi) with load (figure B-10).

e. F/A measurements and ϕ. An accurate measurement of the fuel flow and of the air flow is required during data acquisition to ensure reasonable results are obtained for the heat release analysis. The first step is to determine fuel flow versus fuel dial settings at different speeds. Initial plots were made by running the engine, injecting the fuel into a clean container, and

measuring the fuel flow rate at various speed and fuel flow settings. Then as data is collected, additional fuel flow rates at different settings can be collected. The flow rate chart (figure G-3,Appendix G) can be used as an approximate value at which to set the fuel for a desired flow rate.

The fuel flow rate is the basis for heat addition into the engine: heat addition = $\dot{m}_f$ (LHV). It is therefore important to ensure that the measurement of the fuel flow rates is as accurate as possible. Part of the calculation for mass flow rate is to divide the volume flow rate by the density of the fuel at the fuel temperature. The density of the fuel is calculated by using linear curve for the change of specific gravity as a function of temperature as suggested by Bolt, et al (7) and applying that curve to the measured API of the fuel.

The resulting equation is density of indolene:

density = 0.9990[0.7523 + (15.6 - fuel temperature(^{o}C))0.00081]

A measured quantity of fuel was weighed to check the accuracy of the density calculation. At 20^{o}C, the calculated density of indolene is .7480 g/cm^3 and the measured density is: .7455 g/cm^3. The error is less than 0.4 %

The air flow rate is calculated from a measurement by a manometer. The fuel flow rate is measured from a buret graduated in millileters. The ambiant air pressure affects the first while the temperature affects both measurements. The equivalence ratio can be calculated from the measured flows.

Verification of the measured flow ratio is completed by calculating the equivalence ratio based on the exhaust gas anaylsis. After the engine has

stabilized at a set point, the fuel and air flow rates should be measured while simultaneously measuring the exhaust gas constituents. From these measured values, the equivalence ratio is calculated and compared. The error should be less than $\pm$ 3 %. The equivalence ratio calculated from the measured input flow versus the exhaust gas cart anaylsis equivalence ratio have been plotted (figure B-11). The calculated exhaust ϕ compares favorably with the calculated input ϕ for ϕ less than 1.1.

The accuracy of the exhaust gas analysis equipment is checked by plotting the individual exhaust species concentration versus the ideal species concentration as a function of the exhaust equivalence ratio (figure B-12). The equation used to calculate the ideal emissions at the equivalence ratio ϕ is:

$$C_7H_{11.83} + \frac{9.9575}{\phi} (O_2 + 3.76\ N_2) \quad \text{---->}$$
$$a\ CO_2 + b\ H_2O + c\ CO_2 + d\ H_2 + \frac{37.44}{\phi}\ N_2$$

The ratio of carbon monoxide to hydrogen was assumed to be three: C = 3d. Carbon and hydrogen balance results in these equations:

$$a + c = 7$$

$$2b + 2d = 11.83$$

$$\frac{9.9575}{\phi} = 2a + b + c$$

Solving these last four equations simultaneously at a chosen ϕ yields the ideal emissions at that equivalence ratio.

A more complete check is to use the ratio:

$$\frac{[CO]\,[H_2O]}{[H_2]\,[CO_2]} = 3.5$$

to compute the ideal emission versus ϕ. Also a calculation can be made where the measured carbon monoxide and the measured oxygen can be combined and compared to the ideal emissions by a carbon atom count. These last two checks were not completed for this analysis.

CHAPTER FOUR

ANALYSIS, RESULTS, AND DISCUSSION

4.1 COMPUTER PROGRAM

The computer program used for the heat release analysis is the computer program called QCAL at the MIT Sloan Automotive Lab started by A.Giovanetti(8) and developed by J. Gatowski. The program was developed using a one zone model for the gas in the cylinder. It has been developed to be compatible with the SLN data acquisition program at MIT Sloan Automotive Lab.

The heat release program calculates the mass of gas introduced into the cylinder. It smooths the pressure data curve and calculates the differential pressure change (dp) for each time step. It provides the choice of individual cycle analysis or of average cycle analysis. It calculates the instantaneous heat transfer to the walls, the work done in the cylinder against the piston and corrects for the flow into the crevice and for the crevice heat loss. It then integrates these values to find the combustion heat release as detailed in sections 2-1 and 2-6.

The computer program requires the motored engine data file and the fired engine data file as inputs. It prints a summary file with a list of engine data, environmental conditions and heat release inputs that can be modified for the present run. The output of the program is:

(1) a printed summary listing the inputs used and the heat release values calculated,

(2) a plot file of the combustion heat release, and

(3) a plot file of the energy in the cylinder modified by the mass effects.

4.2 CALIBRATION OF THE MODEL

1. Variations of the Model Parameters. There are seven variables that are required as inputs to the heat release program. These are: C_1, C_2, V_{cr}, V_c, γ, T_w, and the exponent (n) in the heat transfer equation (section 2.3). Two of these, V_c and γ, can be calculated prior to the heat release analysis. V_c can be calculated from the engine dimensions or can be approximated from the compression ratio by using the relationships $V_c + V_D = V_T$ and $V_T/V_c = r_c$ to get:

$$V_c = \frac{V_D}{r_c - 1}$$

where V_c is the clearance volume, V_D the displacement, V_T the volume at BC and r_c the compression ratio (equal to 8.41 : 1). γ is calculated as shown in section 2.4.

a. Changing C_1 Increasing C_1 causes the heat transfer to increase as $Q = C_1 hA\Delta T$. If the heat transfer is estimated to be larger than the actual heat transfer, then the combustion heat release will continue to rise after combustion has been completed. Therefore, the end slope of the combustion heat release profile increases (figure C-1 Appendix C).

b. Changing C_2 Increasing C_2 increases the heat transfer during combustion and expansion. A greater heat transfer to the walls during combustion forces the combustion heat release during combustion to increase.

The result is a large increase in the total value of combustion heat release (figure C-2 Appendix C).

c. Changing V_{cr} The effect of crevice volume as detailed in section 2.2 is both mass and energy loss from the control volume. The increased loss to the crevice due to an increase in the crevice size, results in a small increase of the value of the combustion heat release over the entire combustion heat release curve and a drop in the total energy in the cylinder, especially during the high pressure portion of the engine cycle (figure C-3 Appendix C).

d. Changing T_w Changing the wall temperature over a plausible range has a small effect on the combustion heat release. As T_w increases, the temperature difference between the gas and the walls decrease resulting in a decrease in the heat transfer after combustion. An increase in T_w causes a small decrease in the slope at the end of the combustion heat release curve (figure C-4 Appendix C).

e. Changing the exponent Woschni's heat transfer correlation was rewritten in section 2.3 to incorporate an exponent (n) that could be varied while maintaining the relationships between B, P, T and W. The affect of changing n is opposite to the affect of changing both C_1 and C_2. Decreasing n increases the heat transfer, thus the combustion heat release curve displays an increase in heat release during combustion and an increase after combustion (figure C-5 Appendix C).

The reference pressure used is the intake pressure. The intake pressure has only a small affect on the combustion heat release curve when the pressure

used in calculations is near the correct intake pressure. However, a large error in the intake pressure presents itself as a change in the slope of the combustion heat release curve before and after combustion. As the value for P_I used in the analysis increases, the slope before combustion decreases and the slope after combustion increases (figure C-6 Appendix C).

2. Best Fit of the Model Parameters The data for one engine operating set point was initially chosen for testing in the heat release analysis to determine the correct model parameters. The original setpoint chosen was 1500 RPM with P_I=0.35 atm. The parameters listed in section 4.2.1 were varied in the order detailed there to determine the set of parameters that yielded the desired combustion heat release profile. The profile sought was flat with zero value before combustion, nearly flat after combustion, and approached but did not exceed the energy in the cylinder curve. When a set of model parameters was found that sucessfully modeled the data at 1500 RPM with P_I=0.35 atm, the chosen parameters were then checked against the other five sets of data. The model parameters were individually varied for each set of engine data to verify the effects of varying model paramters for that engine data set. The results of varying the parameters were found to be similar for each set of engine data.

The original set of model paramters sucessfully modeled the heat release for all six sets of engine data as determined by a visual qualitative check of the graphs. To check if another set of model parameters would provide a better qualitative fit, the set of chosen parameters were varied and the six sets of data again analyized with the different variables. The data was

compared by speed and load as displayed in the graphs in Appendix F. The new set of graphs obtained from changing the model parameters was compared to the original set of graphs to determine which model provided a better fit. The first chosen sets of parameters continued to provide the best qualitative fit.

A quantitative fit was desired (Appendix E). The fit chosen was to compare the maximum value of the combustion heat release (determined from the heat release analysis) with the chemical energy released value (mass of fuel multiplied by the lower heating value multiplied by the combustion efficiency). The difference between the two values equals the error, e, which was normalized by the chemical energy released value for each curve to remove the effects of speed and load. A least squares error method was used to determine the error for each set of model parameters for the six data sets. This was done by summing the values of the error squared for each of engine data sets and then taking the square root of this summation. The set of model parameters which yields the smallest error for the range of the engine data, is the set of parameters that give the "best fit". Using the best fit set of model parameters results in the combustion heat release curves which provide the closest approach to the chemical energy released lines.

4.3 RESULTS

Graphs displaying the results of the heat release analysis for each of the engine operating points are presented in Appendix D. There are three lines on each of these graphs.

The first of these, which starts near the top on the left edge and runs

horizontal with a dip in the middle, is a line representing the energy in the cylinder, the "cylinder energy" line. This line is the value of the instantaneous mass of fuel in the cylinder multiplied by the lower heating value of the fuel. This line starts out equal to the maximum fuel energy introduced into the cylinder, but then dips as the pressure rises inside the cylinder and forces mass (and therefore energy) out of the cylinder control volume and into the crevice (section 2.2). The value for the line rises in the later part of the curve as mass returns to the cylinder volume from the crevices. The cylinder energy line in the middle portion of the graph where it dips, represents the minimum energy inside the cylinder. This is because some of the mass forced into the crevice may be burned gas and therefore removes less energy than unburned mass when it leaves the cylinder. The right hand end point should not be greater than the left hand end point but may not return to the initial left hand end value due to some mass remaining in the crevice during expansion and due to the crevice heat loss affects (section 2.2).

The second line on the graph, the short horizontal line near the top right hand side, is the "chemical energy released" line. This line represents the maximum value that the combustion heat release curve is expected to achieve. The value for this line is the value of the fuel energy introduced into the cylinder (mass of fuel multiplied by the lower heating value of fuel) multiplied by the combustion efficiency as calculated from the exhaust gas analysis. The combustion efficiency is computed by calculating the chemical energy remaining in the exhaust components of hydrogen, carbon monoxide, and

hydrocarbons, and from these values determine the fraction of the chemical energy introduced into the cylinder that was burned. Values for the combustion efficiency, the fuel energy introduced into the cylinder, and the chemical energy released line are listed in the engine data table (Appendix A). The line for the chemical energy released is the line that the combustion heat release curve should asymptotically approach.

The third line is the combustion heat release profile. This is the line representing the accumulative quantity of energy released by combustion. This line is expected to be flat and equivalent to zero until combustion starts. It is then expected to have a rapid rise over 30-40 degrees of crank angle after which it should again flatten out with a slope of zero and a value equal to the chemical energy released line. Oxidation can occur after combustion and into the exhaust process so that the combustion heat released curve can have a positive end slope. Recombination of exhaust products can occur which would allow the combustion heat release curve to go above the chemical energy released line and allow it (the combustion heat released curve) to have a negative end slope. It should then asymptotically approach the chemical energy released line from above. The combustion heat release curve cannot be greater than the total fuel energy introduced into the cylinder. Ideally, it should not go above either the cylinder energy curve or the chemical energy released line and should asymptotically approach the chemical energy released line as the combustion process completes.

a. 1000 RPM P_I=0.36 atm (Figure D-1B Appendix D). The combustion heat release curve reaches 96 % of the value of the chemical energy released and

92% of the cylinder energy line. The slope after combustion is very flat with a very small turndown of the slope at the end of the combustion heat release curve. This turndown diverges from the chemical energy released line.

b. 1500 RPM P_I=0.35 atm (Figure D-2B Appendix D). The combustion heat release curve reaches 103 % of the fuel energy released curve, 94 % of the cylinder energy curve, and has a positive slope after combustion is complete. This positve slope diverges from the chemical energy released line but the combustion heat release remains within 4 % of the fuel energy released line.

c. 1500 RPM P_I=.44 atm (Figure D-3B Appendix D). The combustion heat release reaches 99 % of the chemical energy released line, 92 % of the cylinder energy curve, and it has a positive slope so that it continues to approach the chemical energy released line. A dip appears in the combustion heat release curve just after combustion is completed.

d. 1500 RPM WOT (Figure D-4B Appendix D). The combustion heat release curve for WOT displays the same general trends as does the 1500 RPM curve with P_I=.44 atm. It reaches 98 % of the chemical energy curve, 94 % of the cylinder energy curve, and has the same dip just after completion of combustion. During the final portion of the combustion heat release curve the slope becomes negative, diverging from but remaining within 4 % of the chemical energy released.

e. 2500 RPM P_I=0.35 atm (Figure D-5B Appendix D). The combustion heat release curve reaches 104 % of the chemical energy released and 95 % of the cylinder energy. The overall shape of the curve is well modeled. The slope of the combustion heat release curve levels off after combustion and tends to

climb slightly at the end. The slope before combustion is equal to zero as is expected for the model, but is offset by approximately 5 Joules. This phenomena was only displayed for this set of engine data.

f. 2500 RPM WOT (Figure D-6B Appendix D). The combustion heat release curve reaches 102% of the chemical energy released line and contacts the curve for energy in the cylinder before it levels off at 98 % of the cylinder energy. Near the end of the curve, the slope is negative and the combustion heat release curve approaches the chemical energy released line. The curve is well modeled except that the slope is greater than zero prior to combustion. Two possiblities indicated are that either too small an inlet pressure was used or too large a crevice volume was used.

4.4 COMPARISONS

The individual curves can be analyized in different ways. The curves of the energy in the cylinder, the chemical energy release, and the combustion heat release are compared versus changing speed at two loads: (a) with inlet pressure at approximately 0.35 atmosphere and (b) at WOT. The curves can also be compared at steady speed with varying looads at 1500 RPM and 2500 RPM.

The comparisons are made by observing the similiarities in the slope of the curves of the combustion heat release as either the speed or the load changes. The shapes should be the same with similar rates of combustion heat release both during combustion and after combustion. The maximum value of each heat release curve should reach approximately the same percentage of its chemical energy released line. The curves can also be compared relative to

the percentage of the cylinder energy that each achieves. In general, each individual curve is well modeled by the heat release analysis and the curves scale well with load and speed.

a. Varying speed at $P_I \approx 0.35$ atm (Figure F-1 Appendix F) As can be seen in the figure, the shape of the curves is very similar. All three combustion heat release curves show a similar rate in the rise of the combustion heat release and have final slopes that are nearly equivalent. The combustion heat release curve at 1500 RPM and 2500 RPM match even better. They are nearly identical and both achieve 104 % of the chemical energy released. They also both reach 94 % of the cylinder energy. The scaling for speed between 1500 RPM and 2500 RPM is ideal in this case.

It is obvious that the timing of the 1000 RPM line was 10-15 degrees of crank angle later than optimum. The shape of the combustion heat release and the cylinder energy curves are similar to those for 1500 RPM and 2500 RPM but have 10-15 degrees phase shift. The 1000 RPM heat release curve achieved a smaller percentage of the chemical energy released and a smaller percentage of the cylinder energy value than did the 1500 RPM and 2500 RPM curves. The difference for 1000 RPM is that ϕ equals 0.96 with η (combustion) equal to 96 % compared to 1.03 and 91 % respectively for the 1500 RPM and 2500 RPM curves.

b. Varying speed at WOT (Figure F-2 Appendix F) The rate of combustion heat release is identical for both 1500 RPM and 2500 RPM. Both have a positive slope after combustion which changes to a negative slope after approximately 100° of crank angle. The energy in the cylinder and the chemical energy released lines increase with speed, but the increase in the combustion

heat release is greater than the increase in the energy supplied (a 7 % increase of combustion heat release versus a 3 % increase in fuel energy). The combustion efficiencies for both cases are identical but the equivalence ratio for 1500 RPM is 2 % greater.

While the overall scaling for speed is generally good, there is a 4 % difference at WOT. One parameter that could be modified to reduce this difference is the wall temperature, which is expected to increase with speed. Modifying the wall temperature for each speed would lower the combustion heat release at 2500 RPM and improve the speed scaling.

c. Varying load at 1500 RPM (Figure F-3 Appendix F) The combustion heat release curves model well for changing load. All these curves start their initial rise at approximately the same crank angle. The higher loads rise faster to achieve the greater combustion heat release in approximately the same number of crank angle degrees as the lighter loads. They all have positive slopes after combustion. The dip in the combustion heat release displayed immediately after combustion completes on the WOT curve, can be seen to a lesser extent at P_I=.44 atm. All three curves achieve approximately 93 % of the cylinder energy. Due to the increasing combustion efficiency with the increasing load, the values of the chemical energy released rise faster than the combustion heat release. The value for each of the combustion heat release varies less than 4 % from its respective chemical energy released line.

d. Varying load at 2500 RPM (Figure F-4 Appendix F) The two combustion heat release curves at P_I=.35 and at WOT, also look similar in appearance.

They both have a slight rise after combustion and end with a small negative slope. Unlike the curves at 1500 RPM, both combustion heat release curves at 2500 RPM extend above the chemical energy released line, but both decrease near the end to reapproach the chemical energy released line. The final values for the combustion heat release curves are within 2 % of the chemical energy released line.

e. General comments (Figure F-5 Appendix F) The heat release analysis successfully models the combustion heat release for the range of engine data checked. The combustion heat release curves are all flat before combustion, then display a large rise for combustion, and then end with a slope approximately equal to zero. The combustion heat release curves reach 92 to 94 % of the energy introduced into the cylinder and are within 4 % of the chemical energy released line.

The scaling with load is very good. The shape of the curves at each load is mirrored at the other loads for that speed. The percentage of the energy introduced into the cylinder that appears in the combustion heat release is consistant throughout the testing load range.

The scaling with speeed is very good at low load with each curve reflecting the other curves at that load. At WOT, the increase in combustion heat release is greater than the increase of the energy introduced into the cylinder. Varying the wall temperature or varying the exponent (in equation 1 section 2.3) may fine tune the scaling with speed.

CHAPTER FIVE

SUMMARY AND CONCLUSION

Engine performance and the details of the engine combustion process can be studied by using measured cylinder pressure at known volumes in a heat release analysis. The heat release analysis uses the First Law of Thermodynamics and the ideal gas law to determine the apparent heat release in the cylinder. Modifying the apparent heat release for heat transfer to the walls and for the effect of mass and energy flows into the crevices, the heat release from combustion can be determined. The equation for the combustion heat release from section 2.6 is:

$$\delta Q_c = \delta Q_w + \frac{\gamma}{\gamma-1} pdV + \frac{1}{\gamma-1} Vdp + \frac{\gamma}{\gamma-1} \frac{T^*}{T_{cr}} V_{cr} dp$$

where δQ_w is the modification for the heat transfer to the walls using Woshni's (1) equation the combination of the second and third terms is the work done in the cylinder against the piston, and the last term is the modification for the crevice effect.

The Ricardo MK III engine was instrumented for data collection and prepared for operation. The engine was operated and the operating parameters were checked for consistancy with satisfactory results. Engine cylinder pressure was measured for both motored and fired conditions at six operating points in the range of 1000 RPM to 2500 RPM and in the load range from intake pressure equal to 0.35 atmosphere to WOT. Forty four cylces of engine pressure data were averaged for each engine operating point and the average

pressure data was used in the Sloan Automotive Laboratory heat release model to determine the combustion heat release profiles. The model parameters listed in section 4.2.1 were scaled to fit the engine data. The value C_1, used to modify the heat transfer relation, was found to be of the order of unity as expected.

The combustion heat release was successfully modeled with one set of model parameters for the range of the data checked. The resulting profiles were flat with a zero value before combustion, they had a rapid rise in heat release during combustion, and they leveled off after combustion at approximately 93 % of the value of the fuel energy introduced into the cylinder. The criteria used to select the best set of model parameters was a least squares error fit to the value of the chemical energy released. The chemical energy released was determined from the combustion inefficiency (calculated from the chemical energy of the measured hydrogen, carbon monoxide and hydrocarbons remaining in the exhaust gas) by multiplying the fuel introduced into the cylinder by the lower heating value of the fuel and by the combustion efficiency (1.0 - inefficiency). The ideal combustion heat release should asymptotically approach the value of the chemical energy released. The selected model parameters provided heat release profiles that were within 4 % of the chemical energy released.

The heat release model is simple to use and provides accurate results for this engine. To use this model for another engine, the model parameters should be rescaled.

REFERENCES

(1) Woschni, G., "A Universally Applicable Equation for the Instantaneous Heat Transfer Coefficient in the Internal Combustion Engine," SAE Paper 670931, 1967.

(2) Mansouri, S.H., and Heywood, J.B., "Correlations for the Viscosity and Prandtl Number of Hydrocarbon - Air Combustion Products," Combustion Science and Technology, Vol. 23., pp. 251-256, 1980.

(3) MIT course 2.615, "Internal Combustion Engines," class notes, Unburned mixture properties chart of sensible enthalpy and internal energy vs. temperature.

(4) Toda, T., Nonira, H., and Kobashi, K., "Evaluation of the Burned Gas Ratio (BGR) as a Predominant Factor to NO_x," SAE Paper 760765, 1976.

(5) French, C.C.J., "A Universal Test Engine for Combustion Research," SAE Paper 830453, 1983.

(6) Lancaster, D.R., Krieger, R.B., and Lienech, J.H., "Measurement and Analysis of Engine Pressure Data," SAE Paper 750026, 1975.

(7) Bolt, J.A., Derezinski, S.J., and Harrington, D.L., "Influence of Fuel Properties on Metering in Carburetors," SAE Paper 710207, 1971.

(8) Giovanetti, A.J., "Analysis of Hydrocarbon Emissions Mechanisms in a Direct Injection Spark-ignition Engine," Ph.D Thesis, Department of Mechanical Engineering, M.I.T., Cambridge, MA., May 1982.

APPENDIX A

ENGINE DATA SUMMARY

Speed (RPM)	1000	1500	1500	1500	2500	2500
Intake pressure (atm)	0.36	0.35	0.44	WOT	0.35	WOT
Spark Timing ^{o} BTDC	30	45	40	*22	65	30
Torque lb_f-ft brake/motored	3.2 / -4.4	—	6.0 / -5.2	23.6 / -4.4	3.2 / -6.6	—
IMEP gross (atm)	2.67	2.86	3.67	9.75	2.91	10.42
Fuel Flow (g/s)	0.082	0.126	0.163	0.414	0.215	0.710
Air Flow (g/s)	1.131	1.724	2.300	5.787	2.968	9.927
ϕ (intake)	1.04	1.05	1.02	1.03	1.03	1.04
ϕ (exhaust)	0.95	1.03	1.01	1.00	1.07	0.98
Residual Fraction(%)	17.3	15.1	12.5	8.5	11.2	7.0
Fuel Flow (g/cyc)	0.0099	0.033	0.013	0.010	0.034	0.010
Fuel Energy (J/cyc)	426	435	561	1428	444	1469
η (Combustion) %	96	91	93	96	91	96
Fuel Energy x η_{comb} (J/cyc)	407	397	520	1368	402	1406
Heat Release Q max (J/cyc)	392	411	516	1340	420	1440
Q max (% of intake)	91.9	94.4	92.0	94.1	94.5	98.0
Q max/(FE x η_{comb}) (%)	96.3	103.5	99.2	98.0	104.5	102.4
e(J/cyc)	15.3	-13.9	4.3	28.1	-18.0	-34.0
e norm (%)	3.76	-3.51	0.83	2.06	-4.48	-2.42

* Knock Limited

APPENDIX B

Charts and Graphs	Figure
Ricardo Engine Cross-section	B-1
Ricardo Engine Cross-section	B-2
Engine Geometry and Friction Data	B-3
Fuel Characteristics/Density	B-4
Pressure Transducer Calibration	B-5
Fuel System Schematic	B-6
Phasing P-V Diagram	B-7
PV Diagram (scale and bias)	B-8
IMEP vs Torque MEP	B-9
IMEP, Torgue vs. m_a	B-10
ϕ (intake) versus ϕ (exhaust)	B-11
Emissions versus ϕ (exhaust)	B-12
MBT	B-13

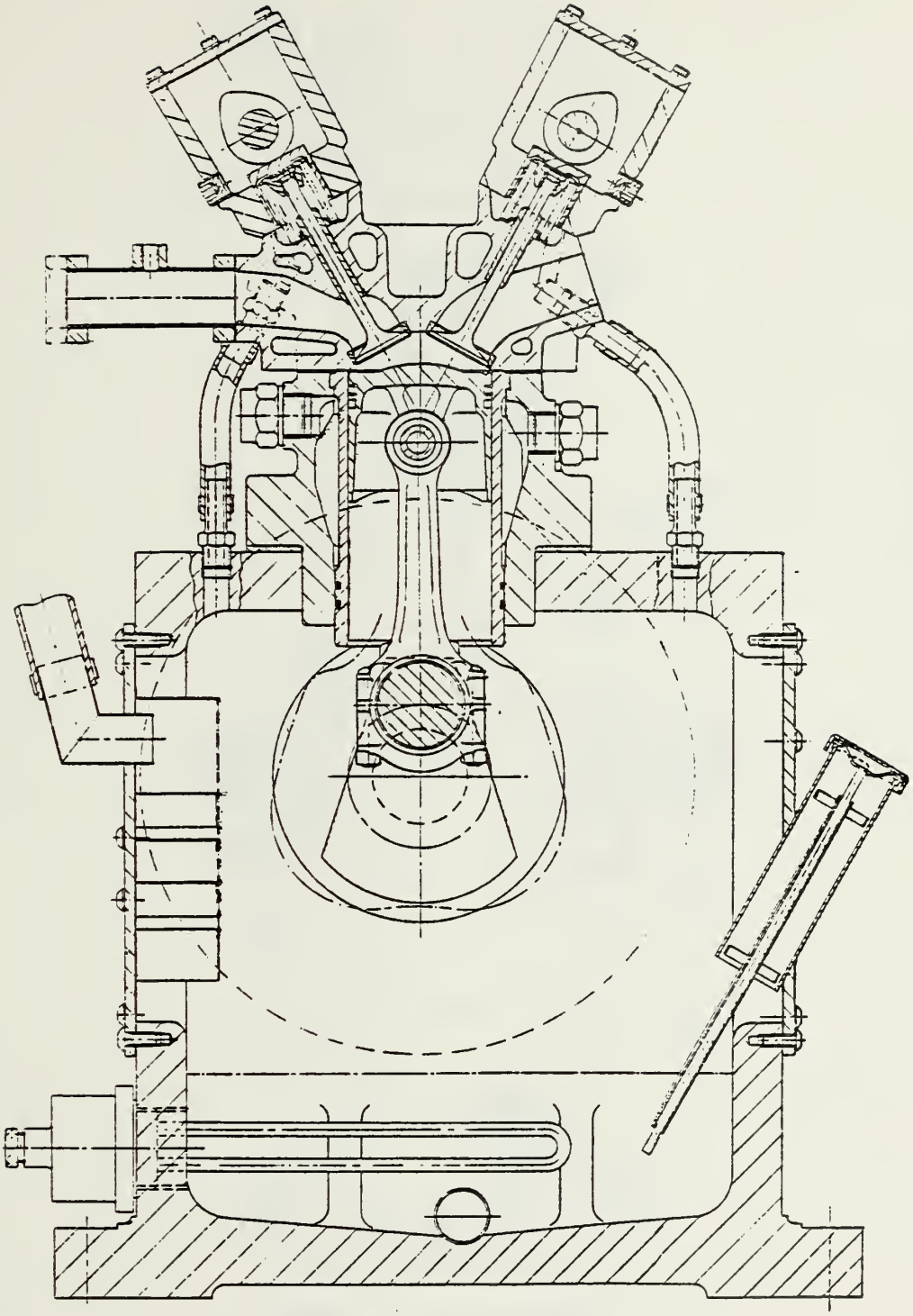

Figure B-1. Ricardo Engine Cross-section

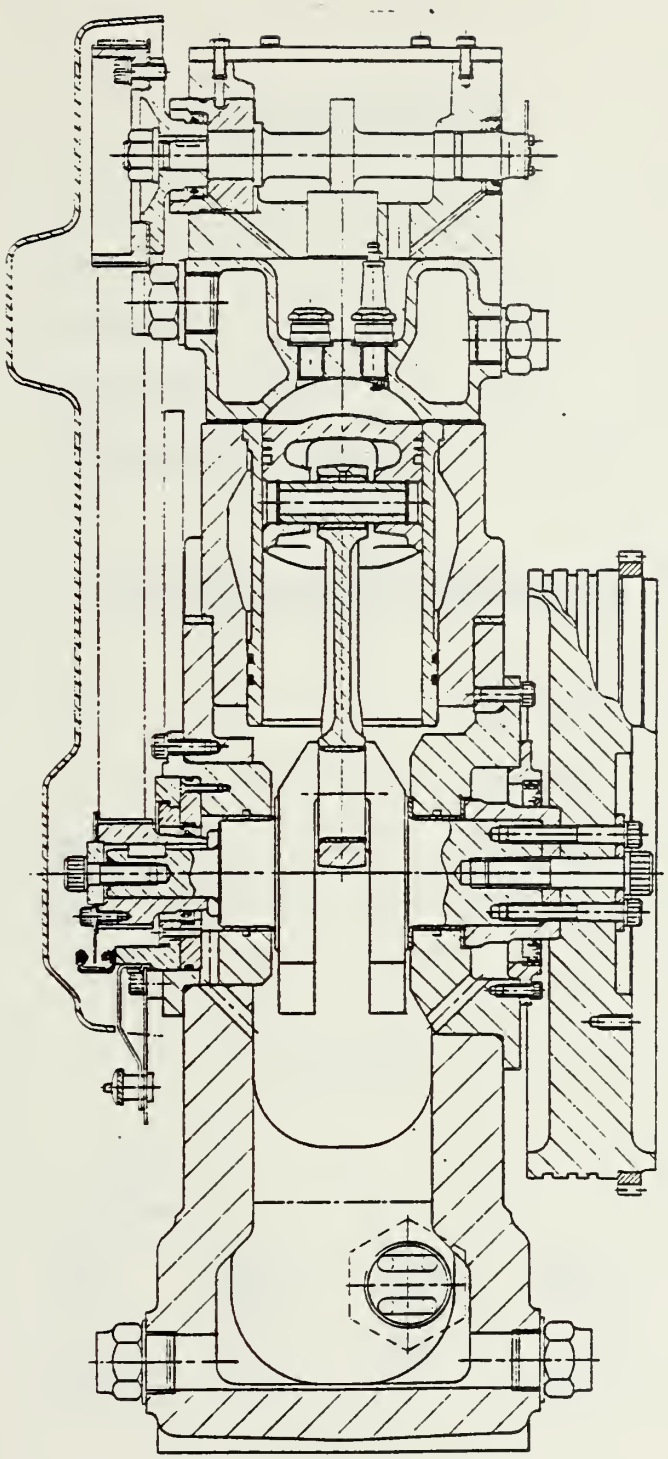

Figure B-2. Ricardo Engine Cross-section

Engine Geometry

Bore	8.57 cm
Stroke	8.6 cm
Compression ratio	8.4 : 1
Correcting rod length	15.79 cm

Valve Opening and Closing Angles

IO	12° BTDC
IC	56° ABDC
EXO	56° BBDC
EXC	12° ATDC

Friction

KW / Rev/sec			
0.9 / 27	1.6 / 38.5	2.2 / 47	3.2 / 57.5
4.4 / 67.5	5.8 / 76	6.9 / 85	8.4 / 95.5

Figure B-3. Engine Geometric and Friction Data

Indolene Characteristics

Hydrogen (% by weight)	12.34
Carbon (% by weight)	86.86
Hydrogen/Carbon ratio based on atomic weight	1.69
Ave. molecular weight($C_7H_{11.83}$)	95.83
Stoichiometric air/fuel ratio	14.37
Lower heating value BTU/lb.	18,562.00
RON	97.2
API gravity	56.6

Density (g/cm^3) of Indolene at Fuel Temperatures (^oC)

$0.999 \times [0.7523 + (15.6 - \text{Fuel Temp}(^oC)) \times 0.00081]$

Temp	Density	Temp	Density
17	.7504	24	.7448
18	.7496	25	.7439
19	.7488	26	.7431
20	.7480	27	.7423
21	,7472	28	.7415
22	.7464	29	.7407
23	.7456	30	.7399

Figure B-4. Indolene Characteristics

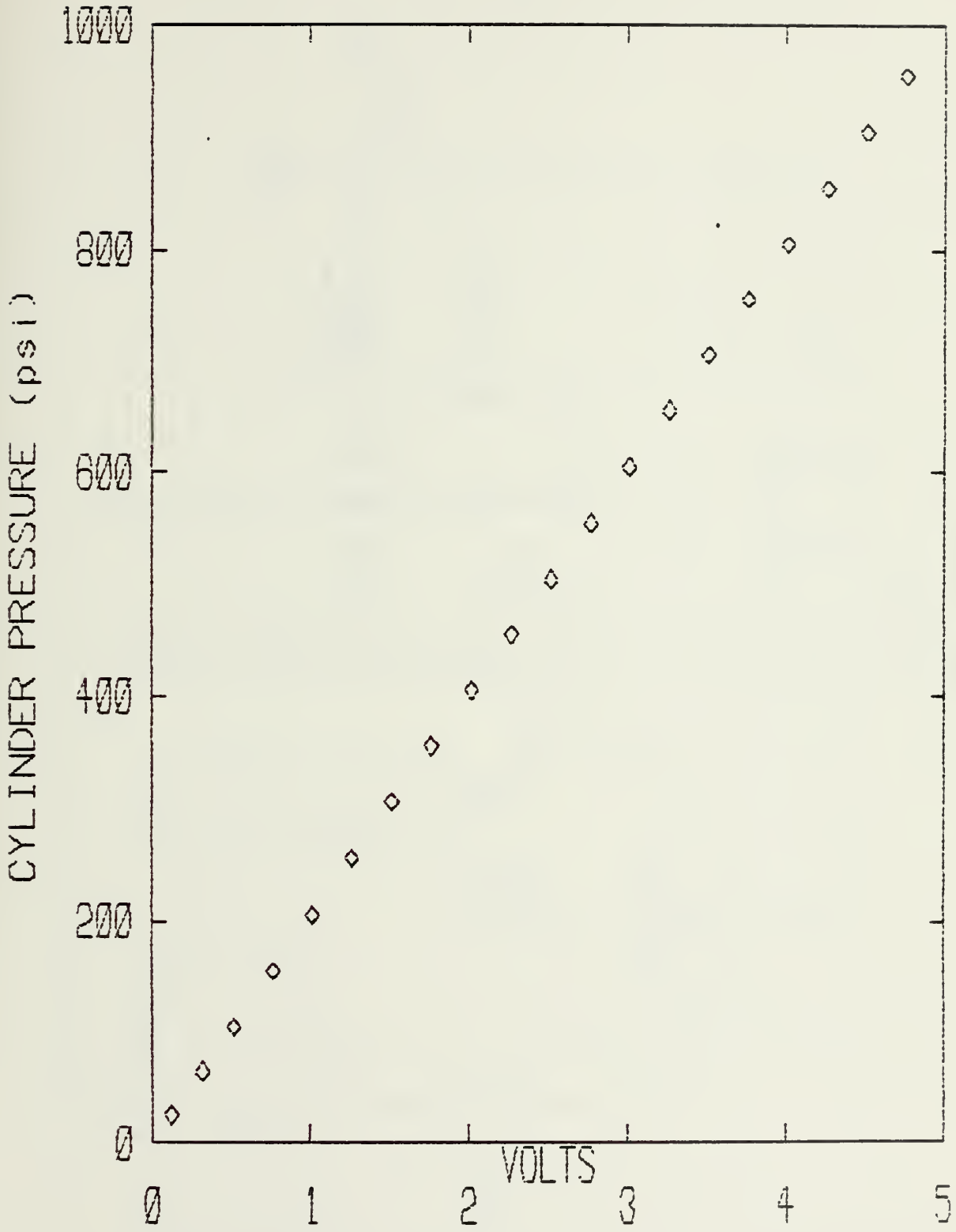

Figure B-5. Pressure Transducer Calibration

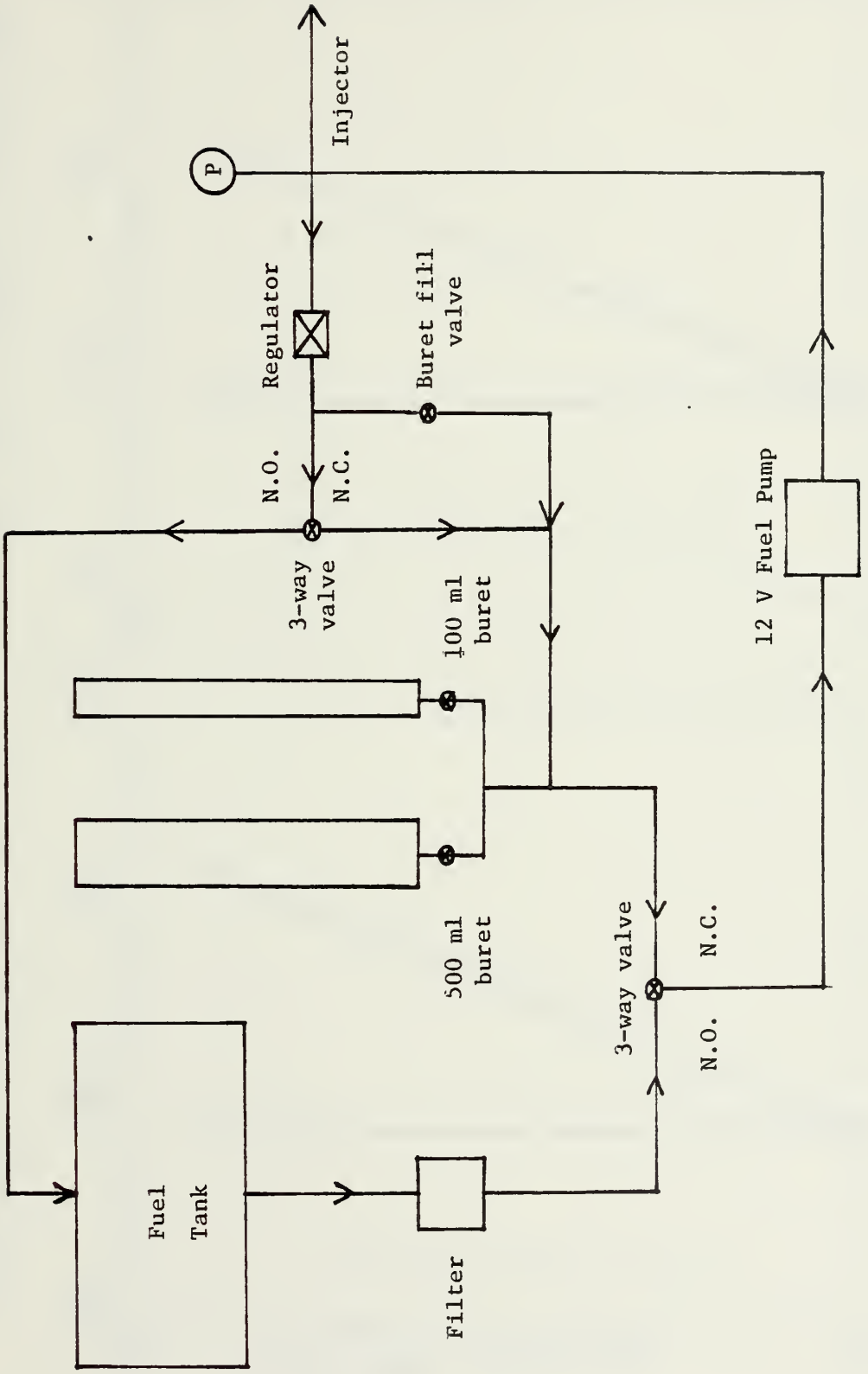

Figure B-6
Fuel System Schematic

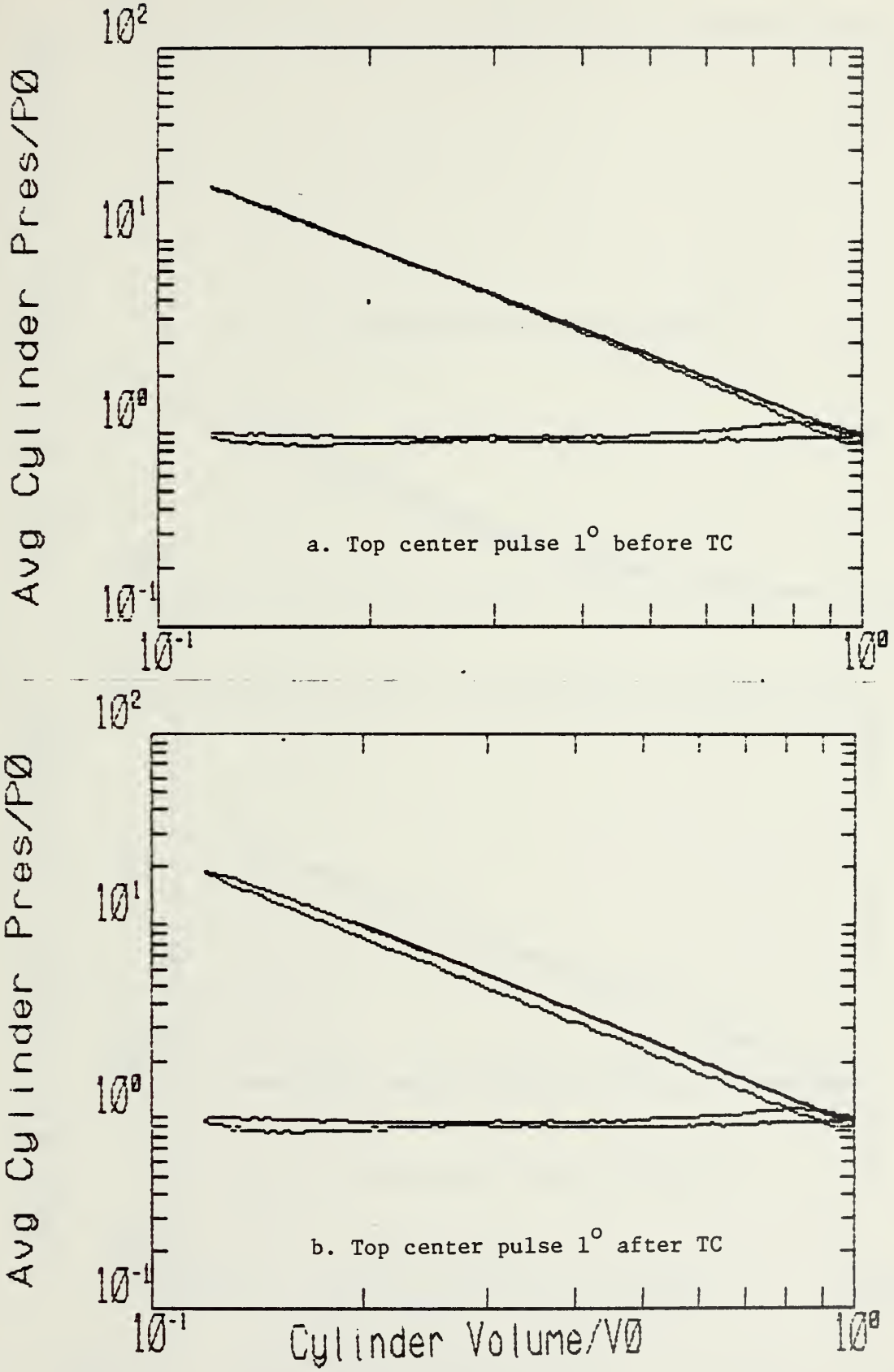

Figure B-7. Verification of Engine Phasing
1500 RPM WOT Motored

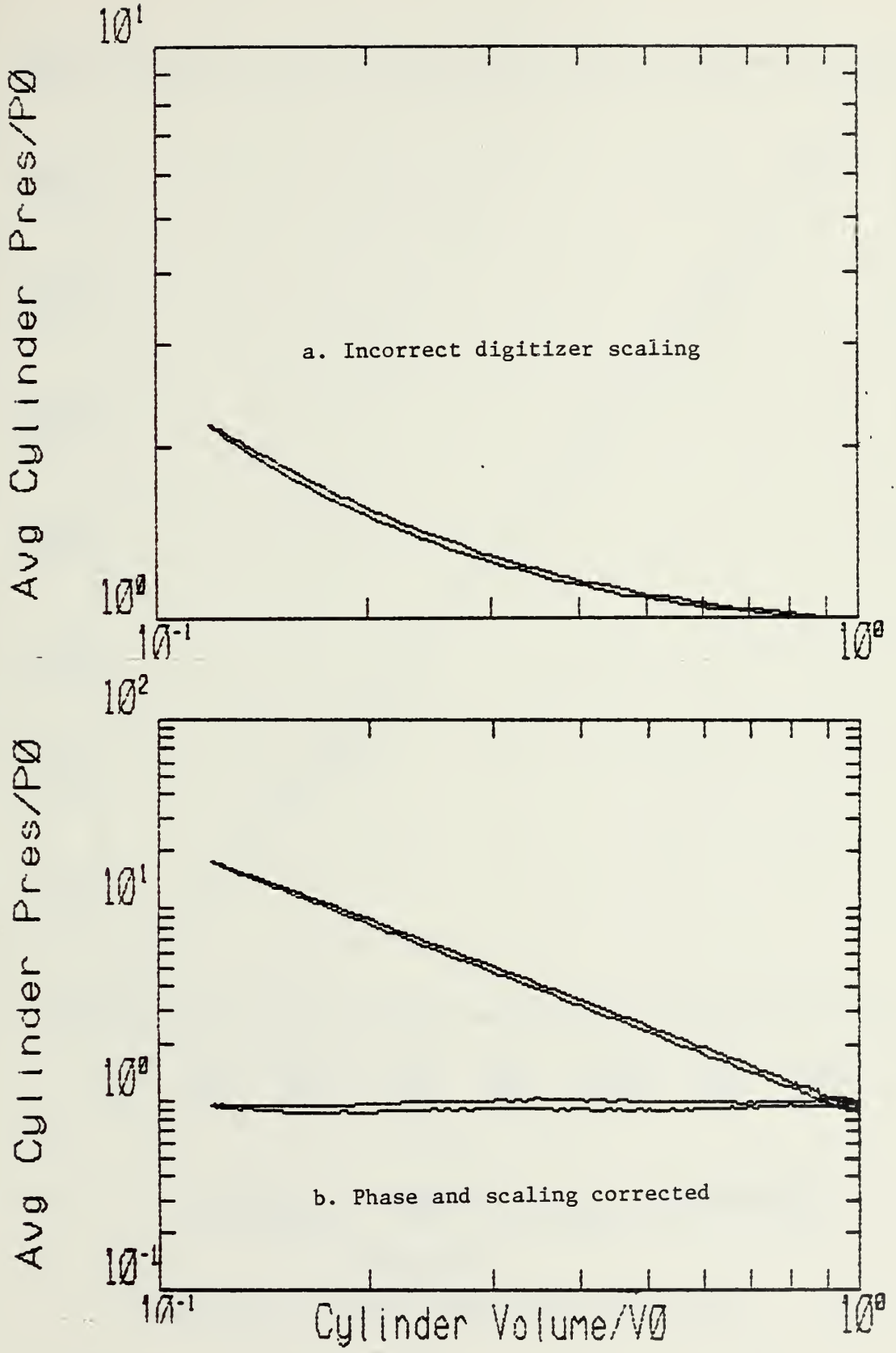

Figure B-8. Verification of engine phasing and digitizer scaling
1500 RPM WOT Motored

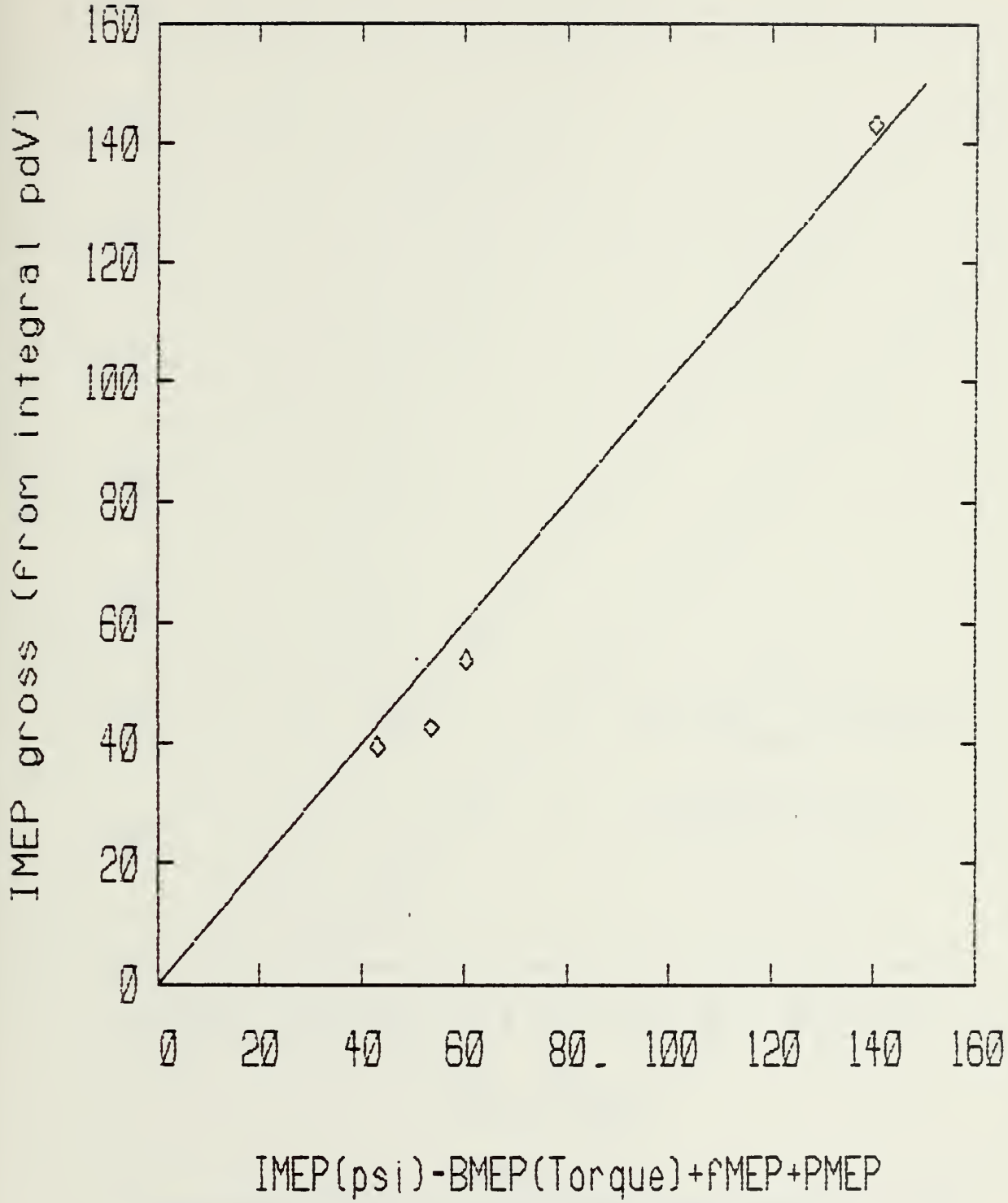

Figure B-9

Verification of engine IMEP versus torque MEP

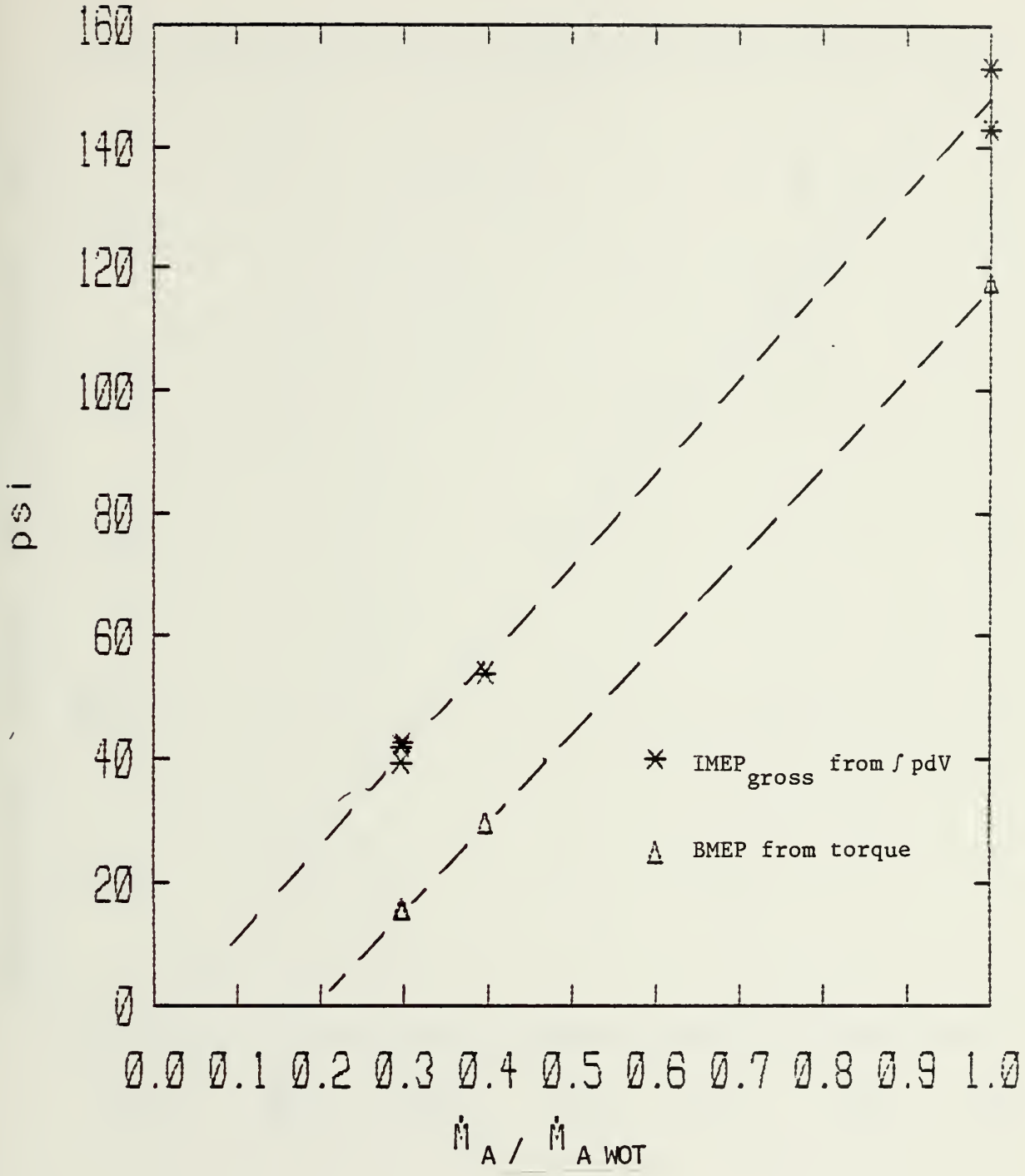

Figure B-10

Comparison of $IMEP_{gross}$ and BMEP (from torque) versus air flow

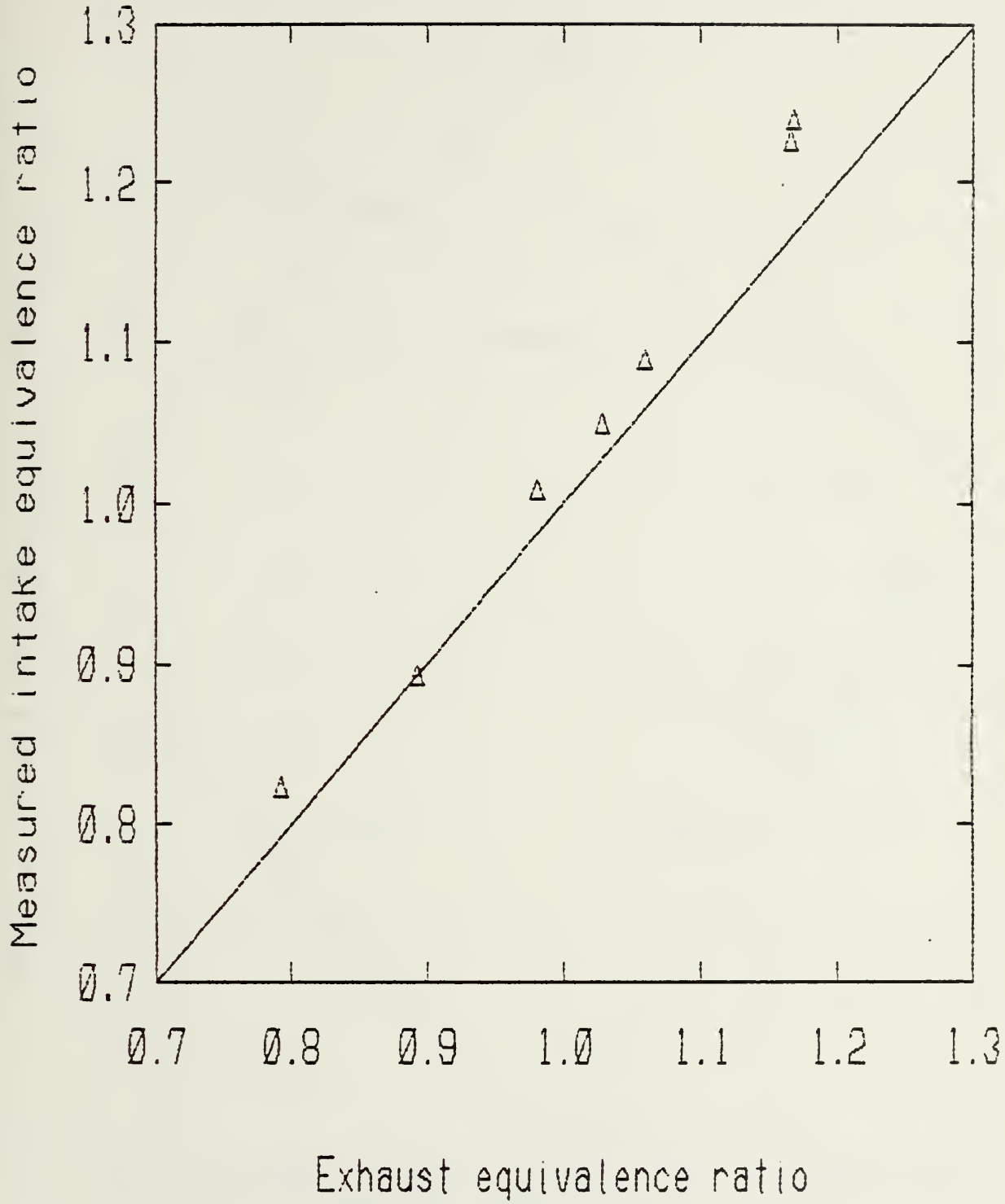

Figure B-11

Comparison of calculate intake equivalence ratio versus exhaust equivalence ratio 1500 RPM P_I=0.35 atm

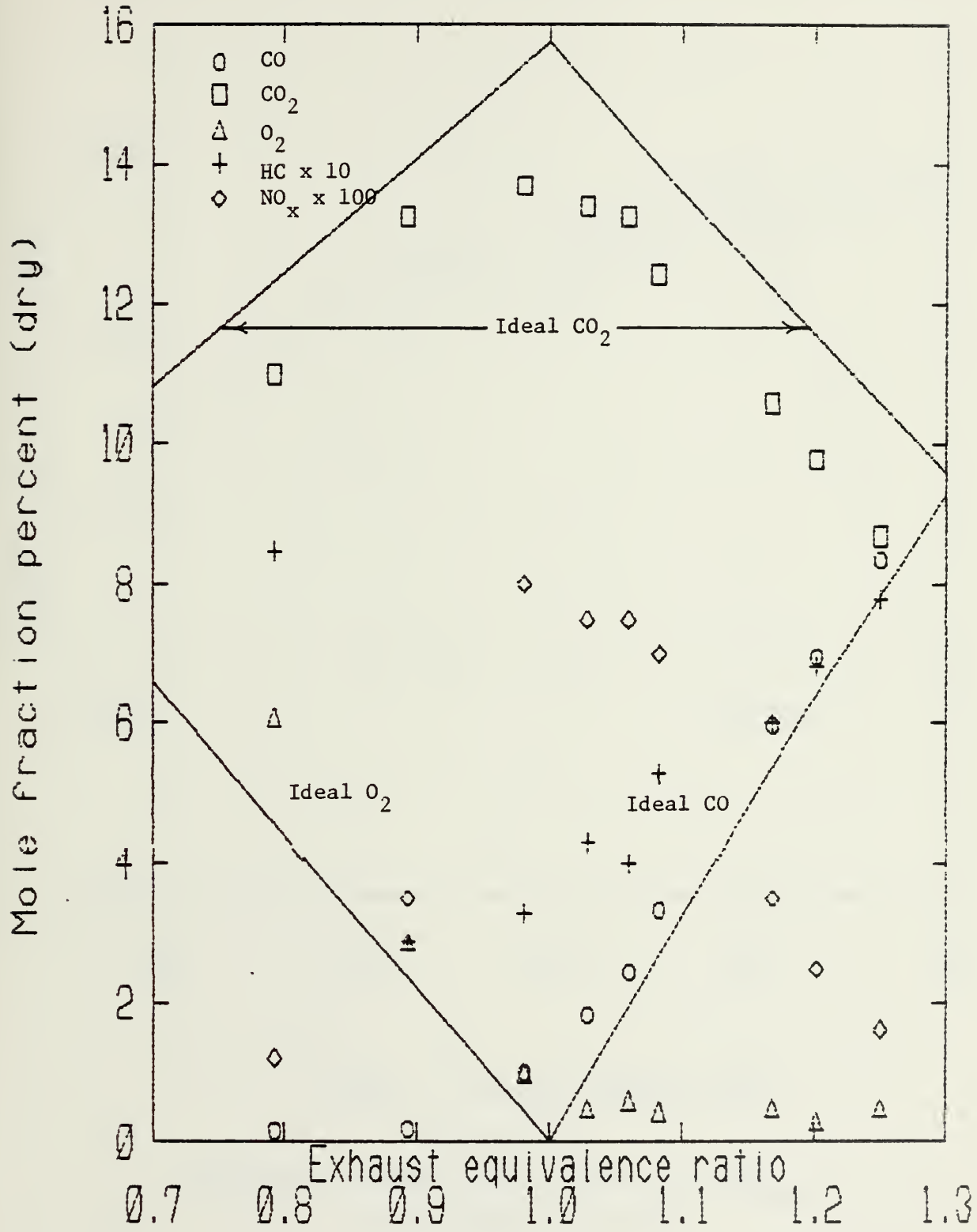

Figure B-i2

Exhaust Emisson check versus ideal exhaust emissons

1500 RPM P_I= 0.35 atm

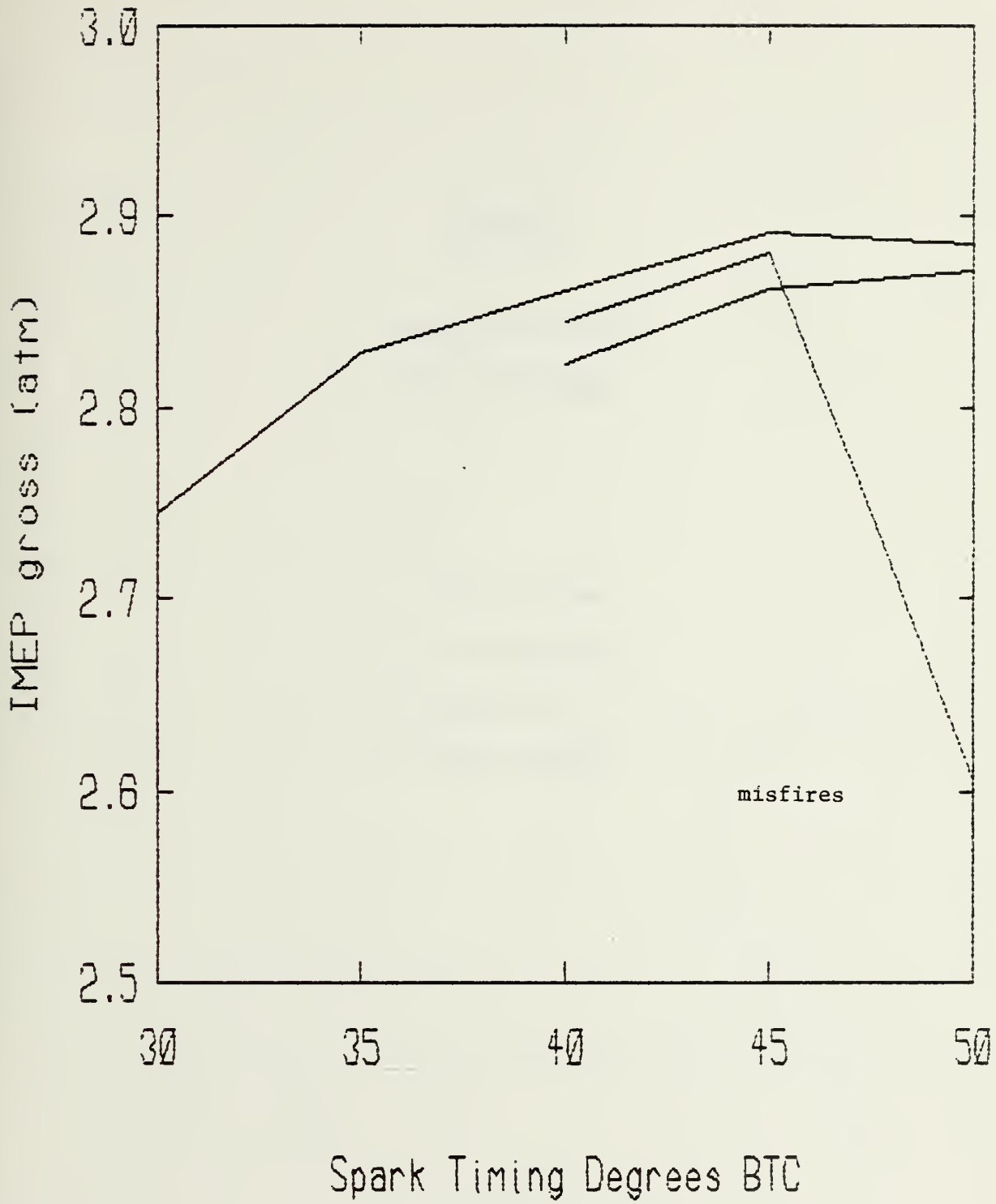

Figure B-13

Determination of MBT using calculation of $IMEP_{gross}$ at 1500 RPM P_I= 0.35 atm

APPENDIX C

AFFECTS OF VARYING MODEL PARAMETERS

1. C_1
2. C_2
3. Crevice Volume
4. Wall Temperature
5. Exponent (n)
6. Intake Pressure

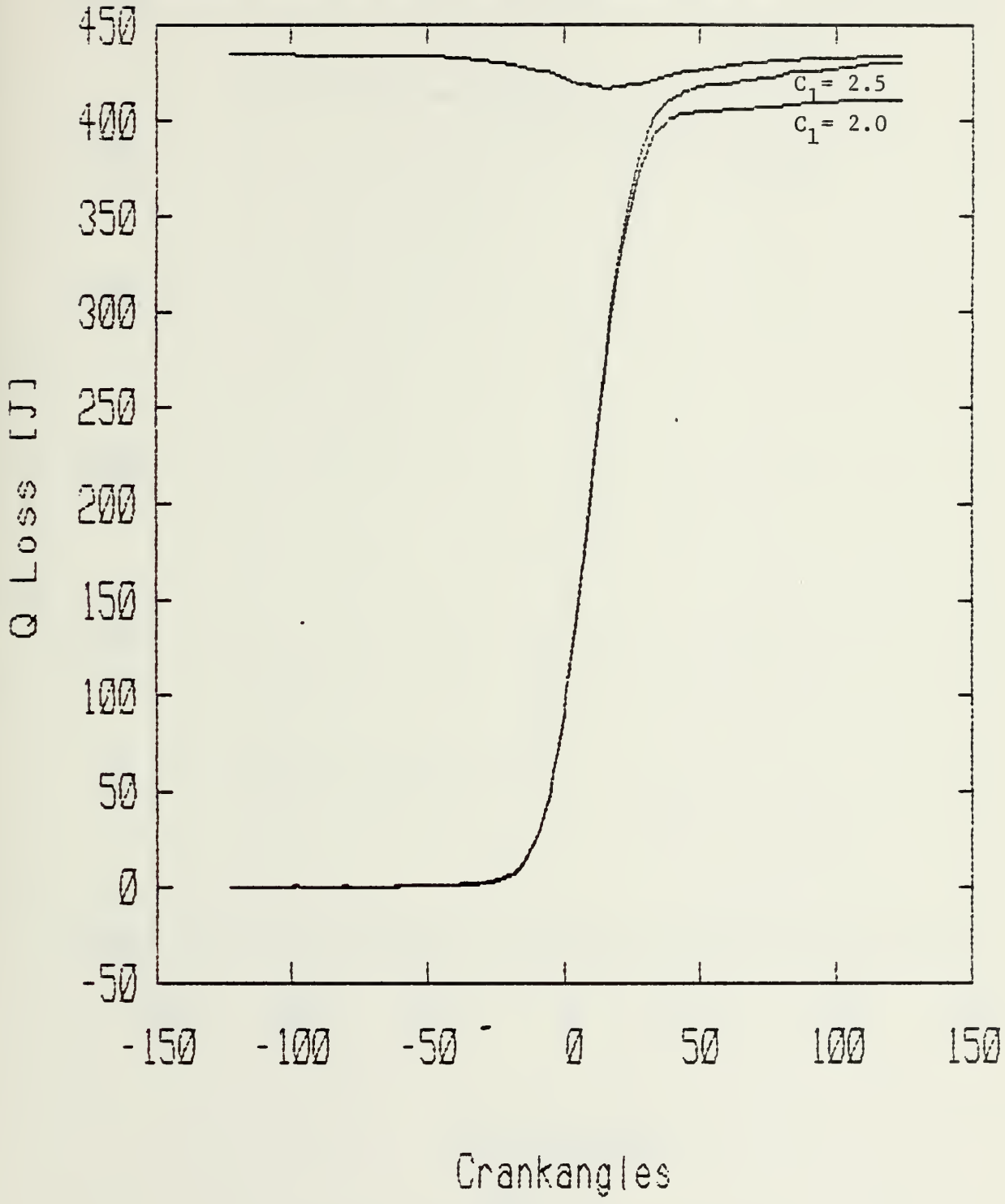

Figure C-1

Affects of changing model parameter C_1

1500 RPM P_I= 0.35 atm

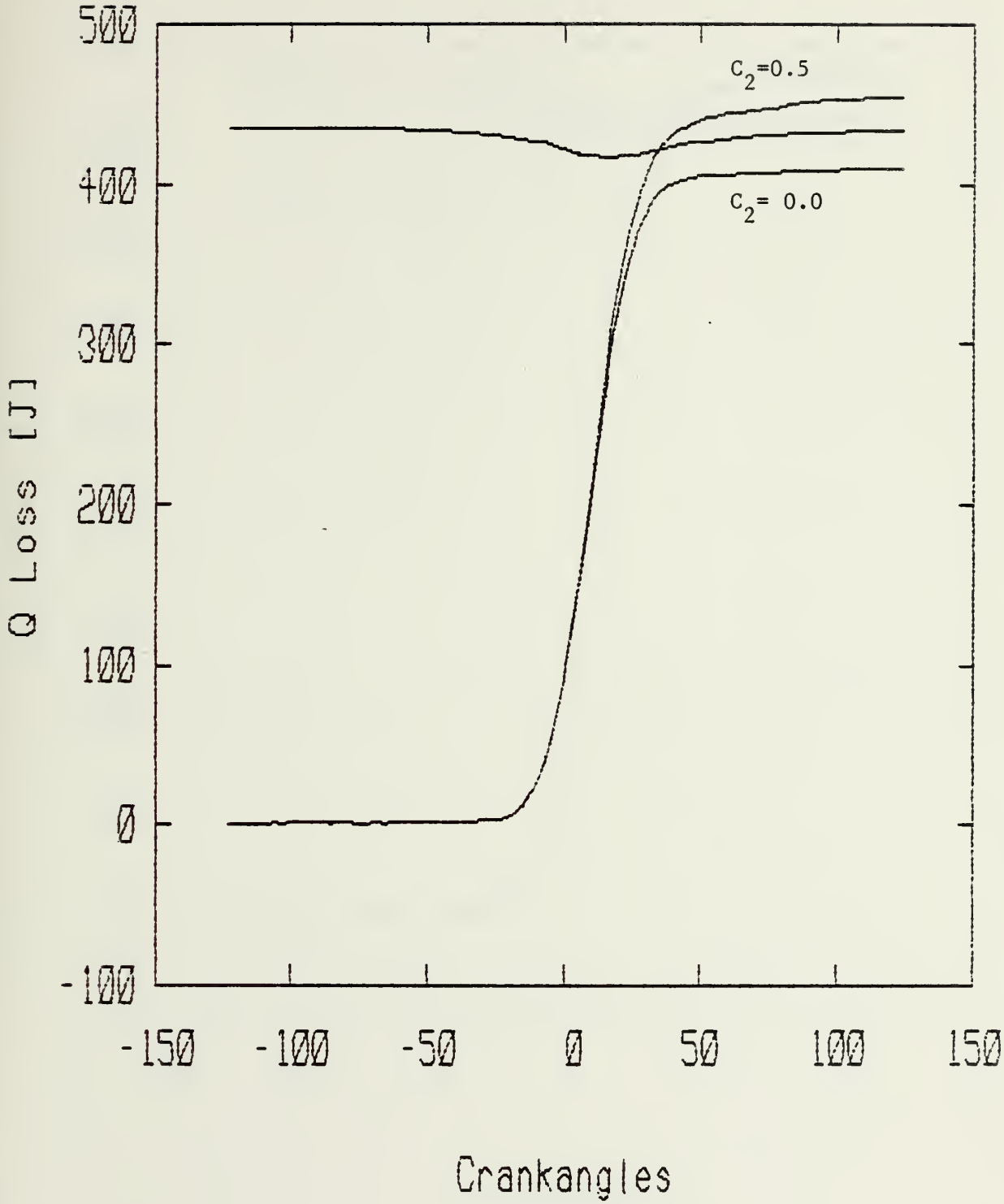

Figure C-2

Affect of changing model parameter C_2

1500 RPM P_I= 0.35 atm

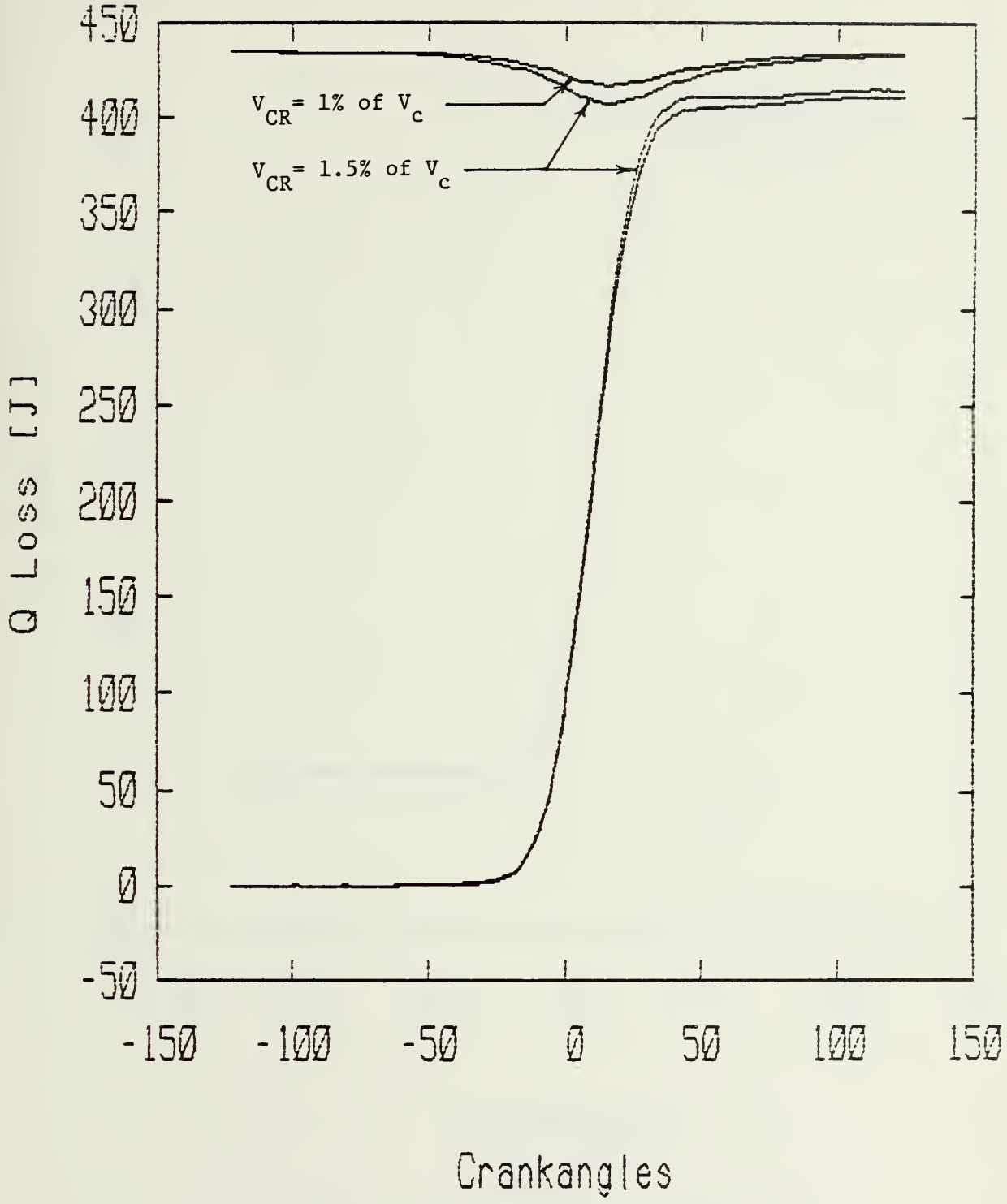

Figure C-3

Affect of changing the crevice volume as a percentage of the clearance volume

1500 RPM P_I= 0.35 atm

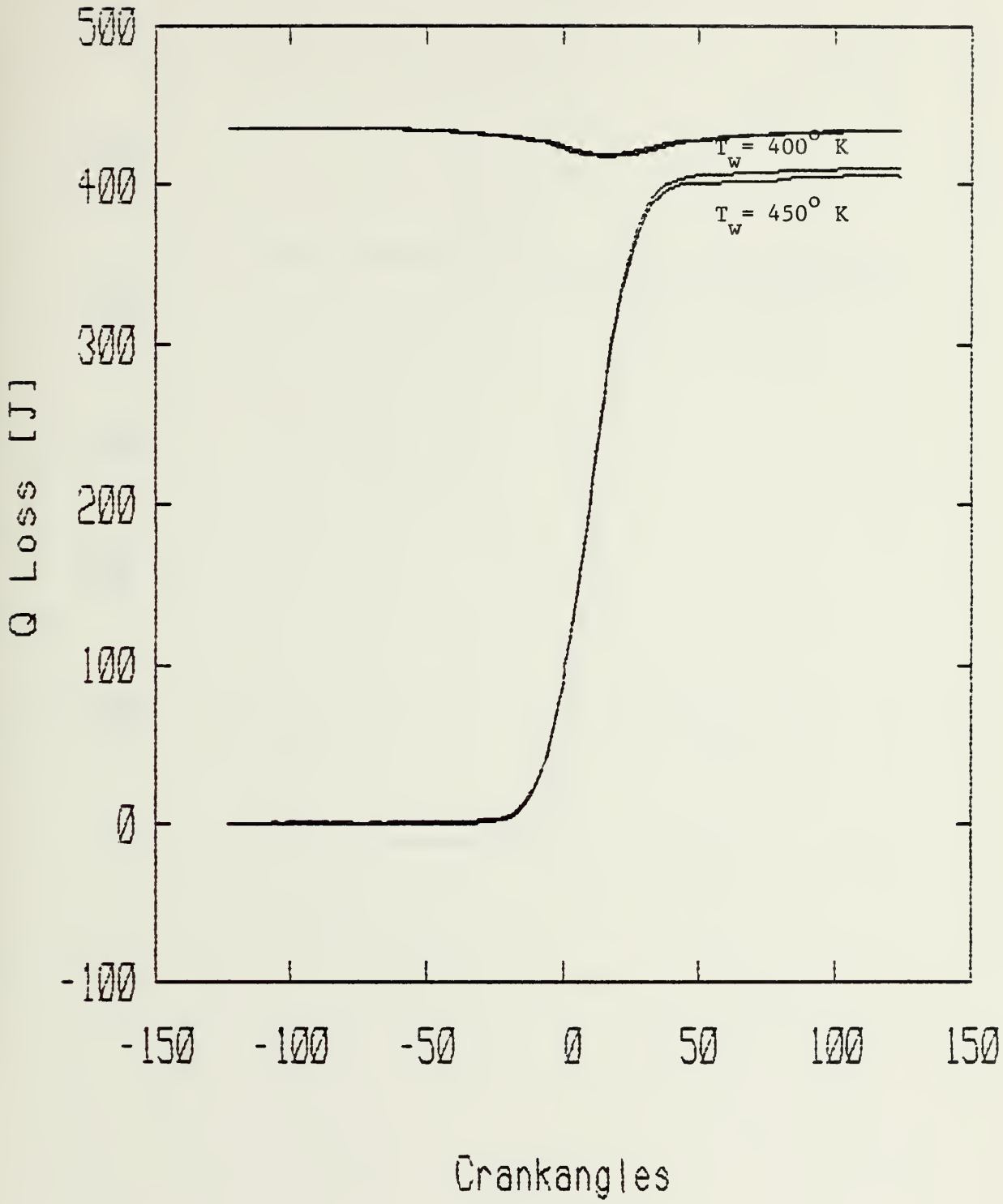

Figure C-4

Affect of Varying wall temperature (T_w)

1500 RPM P_I= 0.35 atm

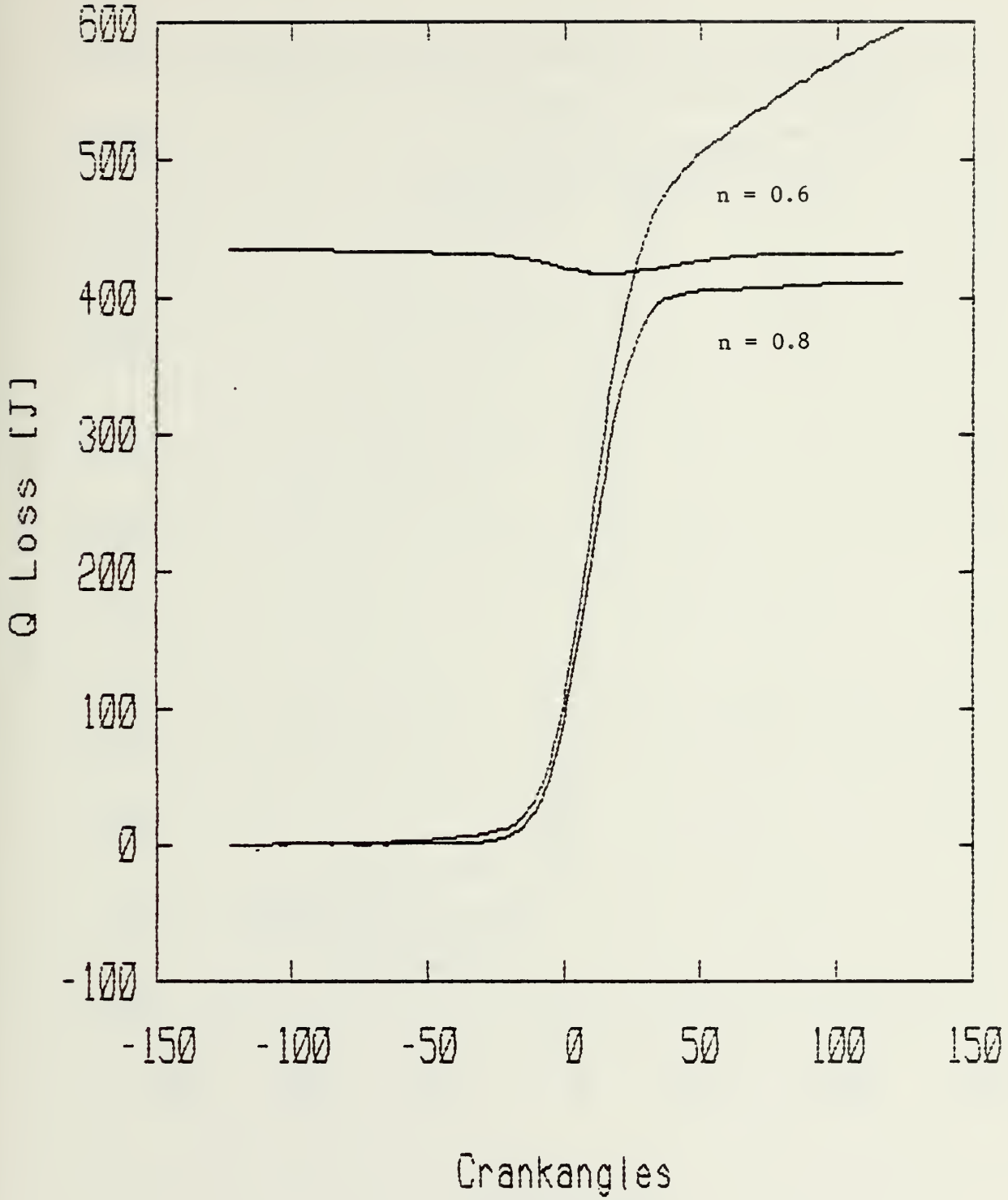

Figure C-5

Affect of changing the exponent (n)

in the heat transfer equation

1500 RPM P_I= 0.35 atm

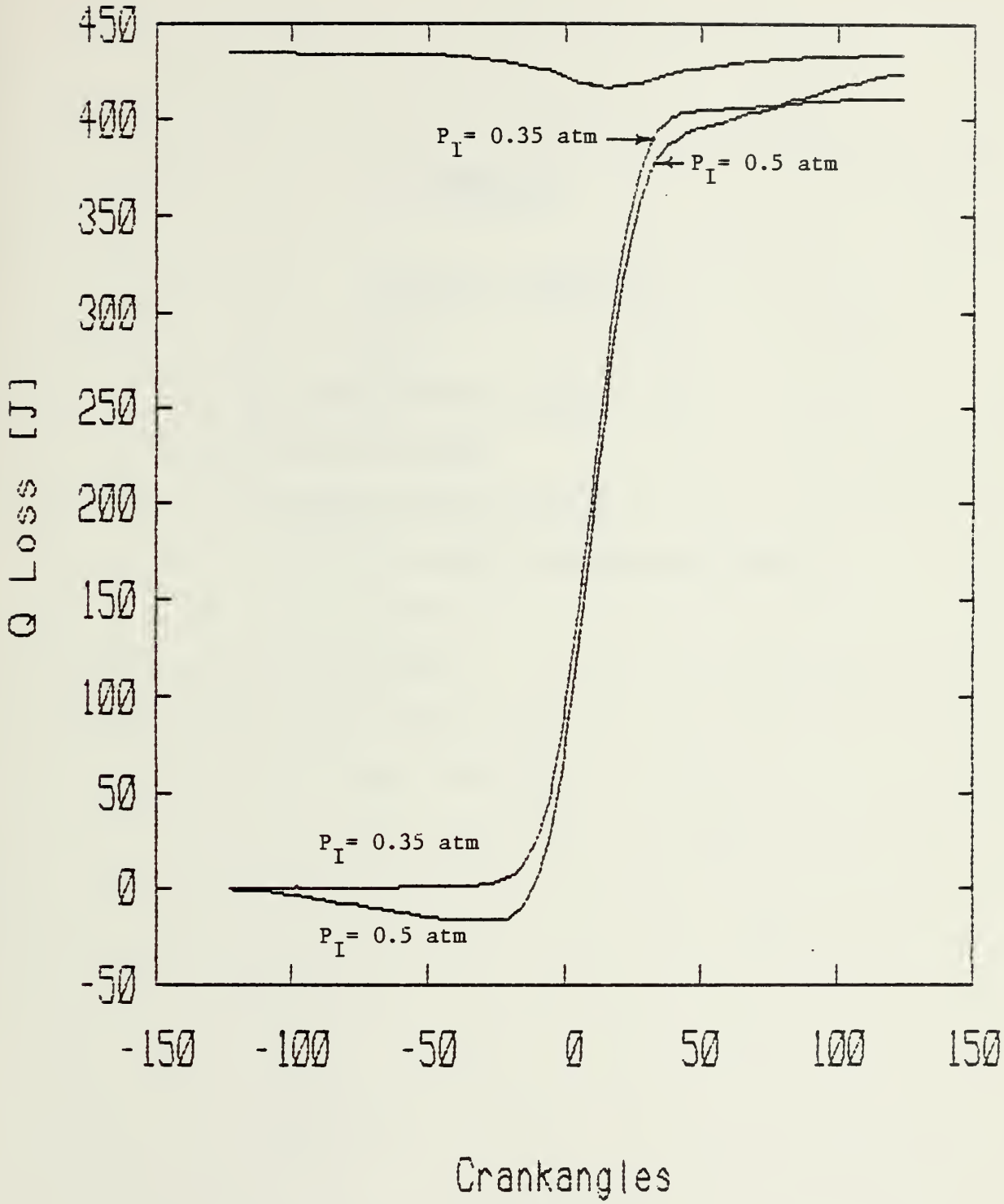

Figure C-6

Affect of varying intake pressure at 1500 RPM

Data from P_I= 0.35 atm .

APPENDIX D

'BEST FIT' GRAPHS OF:

1) Combustion Heat release

2) Cylinder Energy

3) Chemical Energy Released

at the six engine operating points with:

$C_1 = 2.0$

$C_2 = 0.0$

$n = 0.8$

$V_{cr} = 1\ \%$ of V_c

```
Motoring file : RICARDO.24                          43     [a]   1   [b]   43
  Firing file : RICARDO.22                          43     [c]   1   [d]   43

ENGINE RELATED DATA :                    FUEL RELATED DATA :
   [e] Int.Vlv.Cl.=        -124.000          [f]  Fuel Type=        indolene
   [g] Exh.Vlv.Op.=         124.000          [h] LHV [kJ/kg]=       0.431E+05
   [i]  Spark Loc.=         -30.000
   [j] Crev V.[cc]=        0.670E+00

EXPERIMENTAL CONDITIONS :                INPUT VALUES TO ANALYSIS :
   [k] Inl.P.[atm]=           0.356         [l] Area at TDC=          146.600
   [m]        RPM=        1000.000         [n]   Exponent=             0.800
   [o]  Swirl rate=       0.000E+00         [p]  Woshni C1=             2.000
   [q]  Fuel [g/s]=       0.824E-01         [r]  Woshni C2=             0.000
   [s]   Air [g/s]=       0.113E+01         [t] Resid.frac.=           17.300
   [u] Ave. Firing=        Y                [v] Wall tmp[K]=          400.000
   [w] Create Plot=        N
```

H e a t R e l e a s e A n a l y s i s F o r RICARDO ENGINE

A N A L Y S I S F O R A V E R A G E C Y C L E

Total Fuel Energy (J) : 426.257 Total Charge at IVC (G) : 0.176

ANALYSIS OF THE RESULTS FOR THIS CYCLE

Maximum pressure: Pmax=10.170 atm at 23 degrees

Maximum rate of net heat release = 0.123E+02 J/deg at 17 degrees

Maximum rate of gross heat release = 0.131E+02 J/deg at 17 degrees

Maximum gross heat release = 0.392E+03 Joules
i.e: 91.9 % of total energy input, at 102 degrees

* 10% of max at 3 degrees
* 90% of max at 34 degrees

THUS:

Initiation time = 33 degrees
and
Propagation time = 31 degrees

Heat transfer at angle of max Qgross = 0.684E+02 Joules
i.e: 16.0 % of total energy input

Figure D-1A

1000 RPM P_I= 0.36 atm

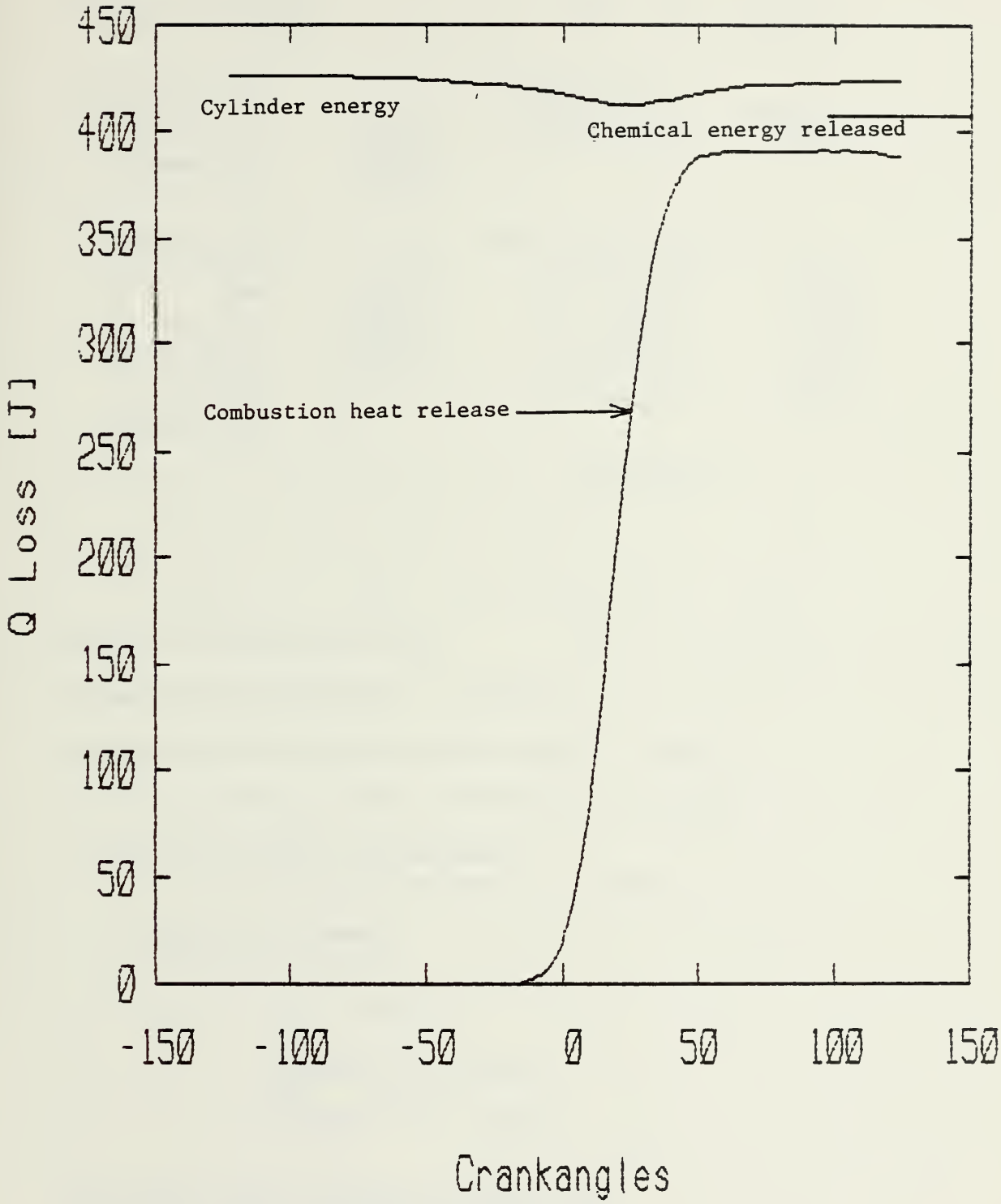

Figure D-1B

1000 RPM P_I= 0.36 atm

```
Motoring file : RICARDO.30                    43    [a]   1   [b]   43
  Firing file : RICARDO.28                    43    [c]   1   [d]   43

ENGINE RELATED DATA :                  FUEL RELATED DATA :
   [e] Int.Vlv.Cl.=       -124.000        [f]  Fuel Type=       indolene
   [g] Exh.Vlv.Op.=        124.000        [h] LHV [kJ/kg]=      0.431E+05
   [i]  Spark Loc.=        -45.000
   [j] Crev V.[cc]=      0.670E+00

EXPERIMENTAL CONDITIONS :              INPUT VALUES TO ANALYSIS :
   [k] Inl.P.[atm]=          0.350        [l] Area at TDC=         146.600
   [m]         RPM=       1500.000        [n]    Exponent=          0.800
   [o]  Swirl rate=      0.000E+00        [p]   Woshni C1=          2.000
   [q]  Fuel [g/s]=      0.126E+00        [r]   Woshni C2=          0.000
   [s]   Air [g/s]=      0.172E+01        [t] Resid.frac.=         15.100
   [u] Ave. Firing=      Y                [v] Wall tmp[K]=        400.000
   [w] Create Plot=      N

H e a t   R e l e a s e   A n a l y s i s   F o r   RICARDO ENGINE

A N A L Y S I S   F O R   A V E R A G E   C Y C L E

Total Fuel Energy (J) :   435.224     Total Charge at IVC (G) :     0.174

ANALYSIS OF THE RESULTS FOR THIS CYCLE

Maximum pressure: Pmax=12.847 atm   at  16 degrees

Maximum rate of net heat release = 0.119E+02 J/deg   at   9 degrees

Maximum rate of gross heat release = 0.130E+02 J/deg   at   9 degrees

Maximum gross heat release = 0.411E+03 Joules
        i.e:  94.4 % of total energy input,   at 114 degrees

     * 10% of max at  -8 degrees
     * 90% of max at  25 degrees

                          THUS:

                  Initiation time =  37 degrees
                  and
                  Propagation time =  33 degrees


Heat transfer at angle of max Qgross = 0.790E+02 Joules
        i.e: 18.1 % of total energy input
```

Figure D-2A

1500 RPM P_I= 0.35 atm

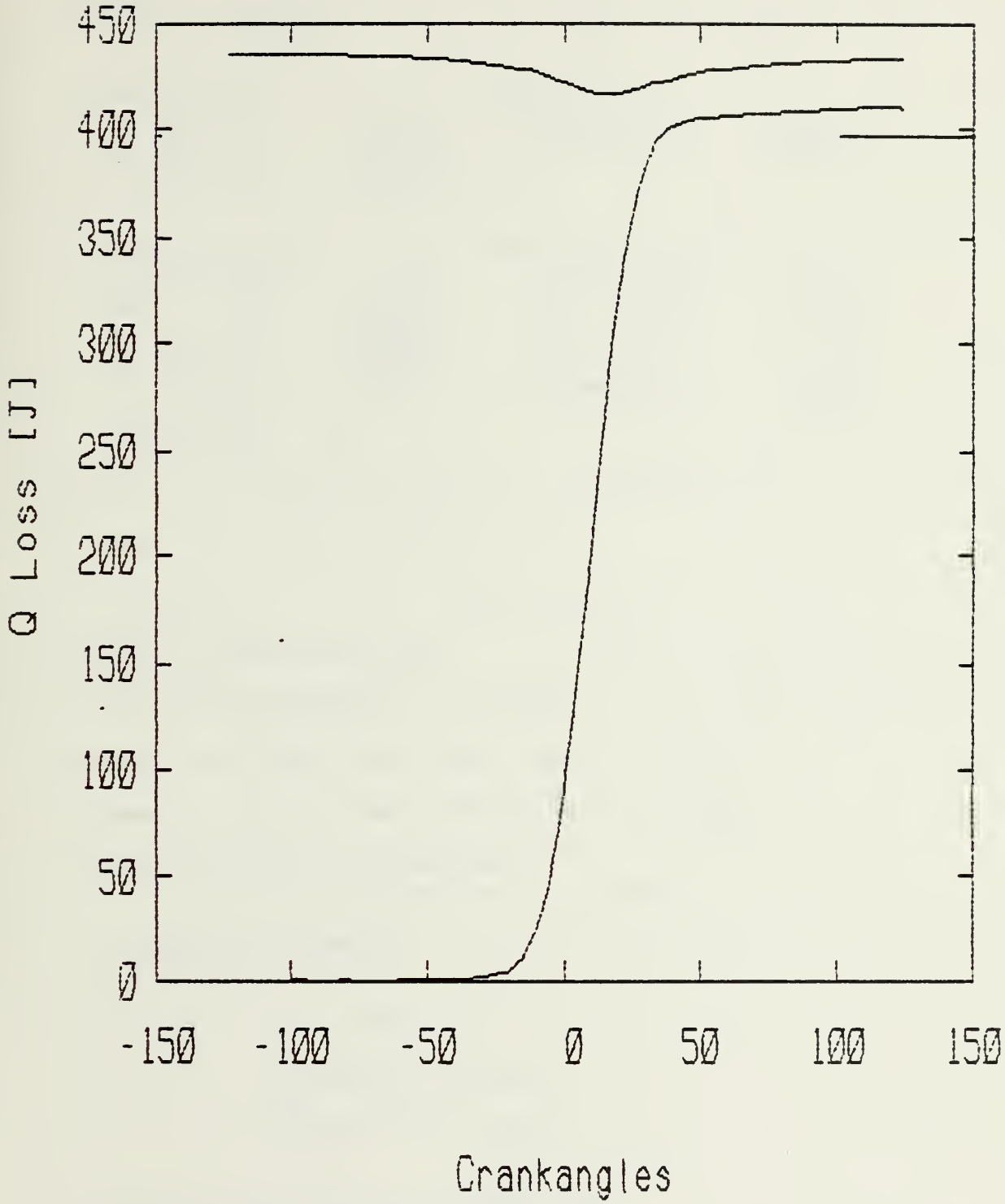

Figure D-2B

1500 RPM P_I=0.35 atm

```
Motoring file : RICARDO.45                          43    [a]   1   [b]   43
  Firing file : RICARDO.43                          43    [c]   1   [d]   43

ENGINE RELATED DATA :                    FUEL RELATED DATA :
   [e] Int.Vlv.Cl.=        -124.000          [f]  Fuel Type=        indolene
   [g] Exh.Vlv.Op.=         124.000          [h] LHV [kJ/kg]=       0.431E+05
   [i]  Spark Loc.=         -40.000
   [j] Crev V.[cc]=        0.670E+00

EXPERIMENTAL CONDITIONS :                INPUT VALUES TO ANALYSIS :
   [k] Inl.P.[atm]=           0.436         [l] Area at TDC=          146.600
   [m]        RPM=        1500.000         [n]    Exponent=            0.800
   [o]  Swirl rate=       0.000E+00        [p]   Woshni C1=            2.000
   [q]  Fuel [g/s]=       0.163E+00        [r]   Woshni C2=            0.000
   [s]   Air [g/s]=       0.230E+01        [t] Resid.frac.=           12.500
   [u] Ave. Firing=       Y                [v] Wall tmp[K]=          400.000
   [w] Create Plot=       N

H e a t   R e l e a s e   A n a l y s i s   F o r   RICARDO ENGINE

A N A L Y S I S   F O R   A V E R A G E   C Y C L E

Total Fuel Energy (J) :   561.101     Total Charge at IVC (G) :      0.225

ANALYSIS OF THE RESULTS FOR THIS CYCLE

Maximum pressure: Pmax=18.825 atm   at  13 degrees

Maximum rate of net heat release = 0.190E+02 J/deg   at   5 degrees

Maximum rate of gross heat release = 0.208E+02 J/deg   at   5 degrees

Maximum gross heat release = 0.516E+03 Joules
         i.e:  92.0 % of total energy input,   at 113 degrees

     * 10% of max at -10 degrees
     * 90% of max at  16 degrees

                              THUS:

                    Initiation time =  30 degrees
                    and
                    Propagation time =  26 degrees


Heat transfer at angle of max Qgross = 0.999E+02 Joules
         i.e: 17.8 % of total energy input
```

Figure D-3A

1500 RPM P_I=0.44 atm

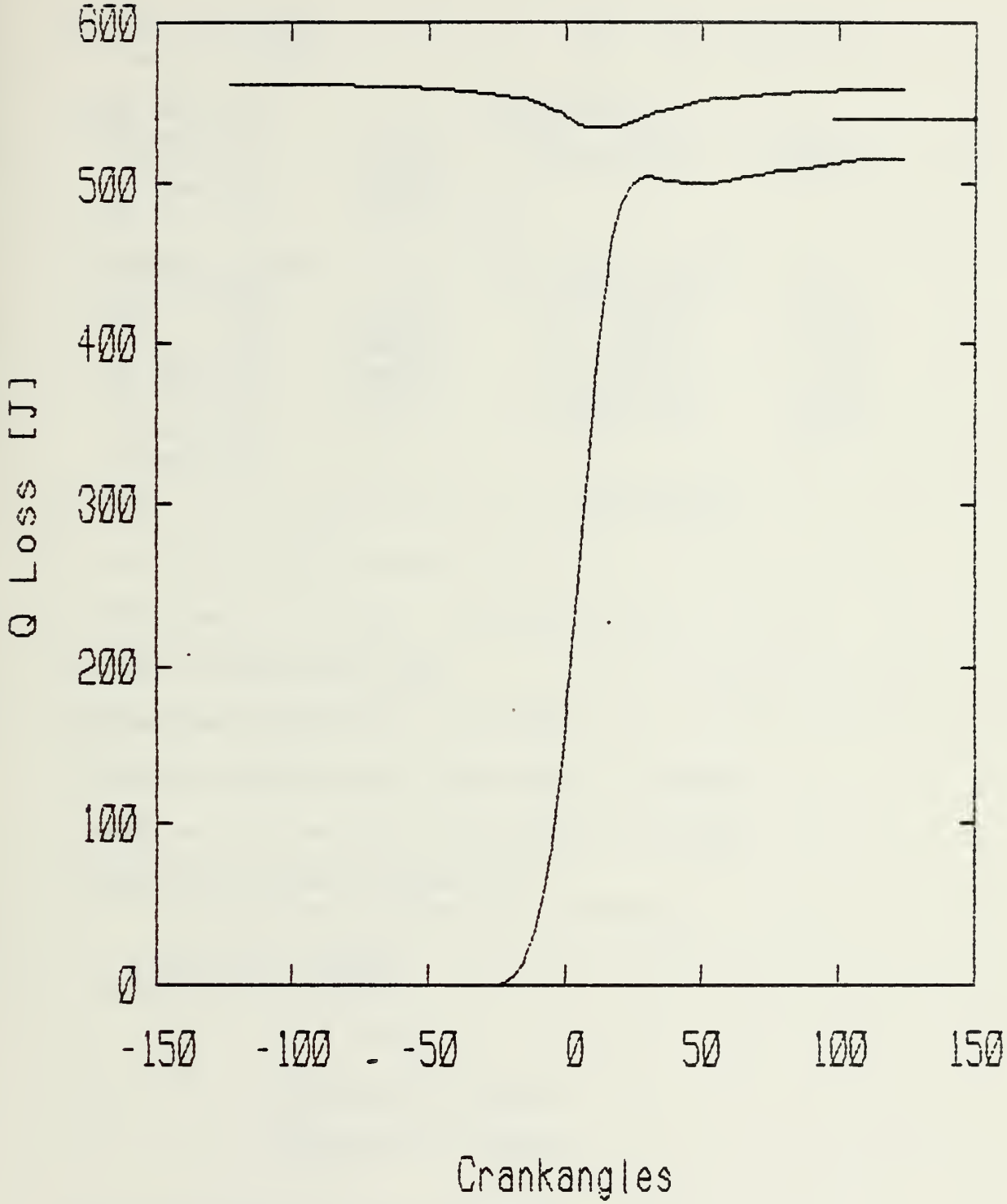

Figure D-3B

1500 RPM P_I= 0.44 atm

```
Motoring file : RICARDO.8                          43    [a]   1   [b]   43
  Firing file : RICARDO.1                          43    [c]   1   [d]   43

ENGINE RELATED DATA :                    FUEL RELATED DATA :
   [e] Int.Vlv.Cl.=        -124.000          [f]  Fuel Type=        indolene
   [g] Exh.Vlv.Op.=         124.000          [h] LHV [kJ/kg]=       0.431E+05
   [i]  Spark Loc.=         -22.000
   [j] Crev V.[cc]=        0.670E+00

EXPERIMENTAL CONDITIONS :                INPUT VALUES TO ANALYSIS :
   [k] Inl.P.[atm]=           1.008          [l] Area at TDC=          146.600
   [m]         RPM=        1500.000          [n]  Exponent=              0.800
   [o]  Swirl rate=       0.000E+00          [p]  Woshni C1=             2.000
   [q]  Fuel [g/s]=       0.414E+00          [r]  Woshni C2=             0.000
   [s]   Air [g/s]=       0.579E+01          [t] Resid.frac.=            8.500
   [u] Ave. Firing=       Y                  [v] Wall tmp[K]=          400.000
   [w] Create Plot=

H e a t   R e l e a s e   A n a l y s i s   F o r   RICARDO ENGINE

A N A L Y S I S   F O R   A V E R A G E   C Y C L E

Total Fuel Energy (J) :  1428.100     Total Charge at IVC (G) :      0.542

ANALYSIS OF THE RESULTS FOR THIS CYCLE

Maximum pressure: Pmax=42.547 atm   at  18 degrees

Maximum rate of net heat release = 0.551E+02 J/deg   at  10 degrees

Maximum rate of gross heat release = 0.590E+02 J/deg   at  10 degrees

Maximum gross heat release = 0.134E+04 Joules
         i.e:  94.1 % of total energy input,   at 100 degrees

     * 10% of max at  -3 degrees
     * 90% of max at  20 degrees

                              THUS:

                    Initiation time =  19 degrees
                    and
                    Propagation time =  23 degrees


Heat transfer at angle of max Qgross = 0.187E+03 Joules
         i.e: 13.1 % of total energy input
```

Figure D-4A

1500 RPM WOT

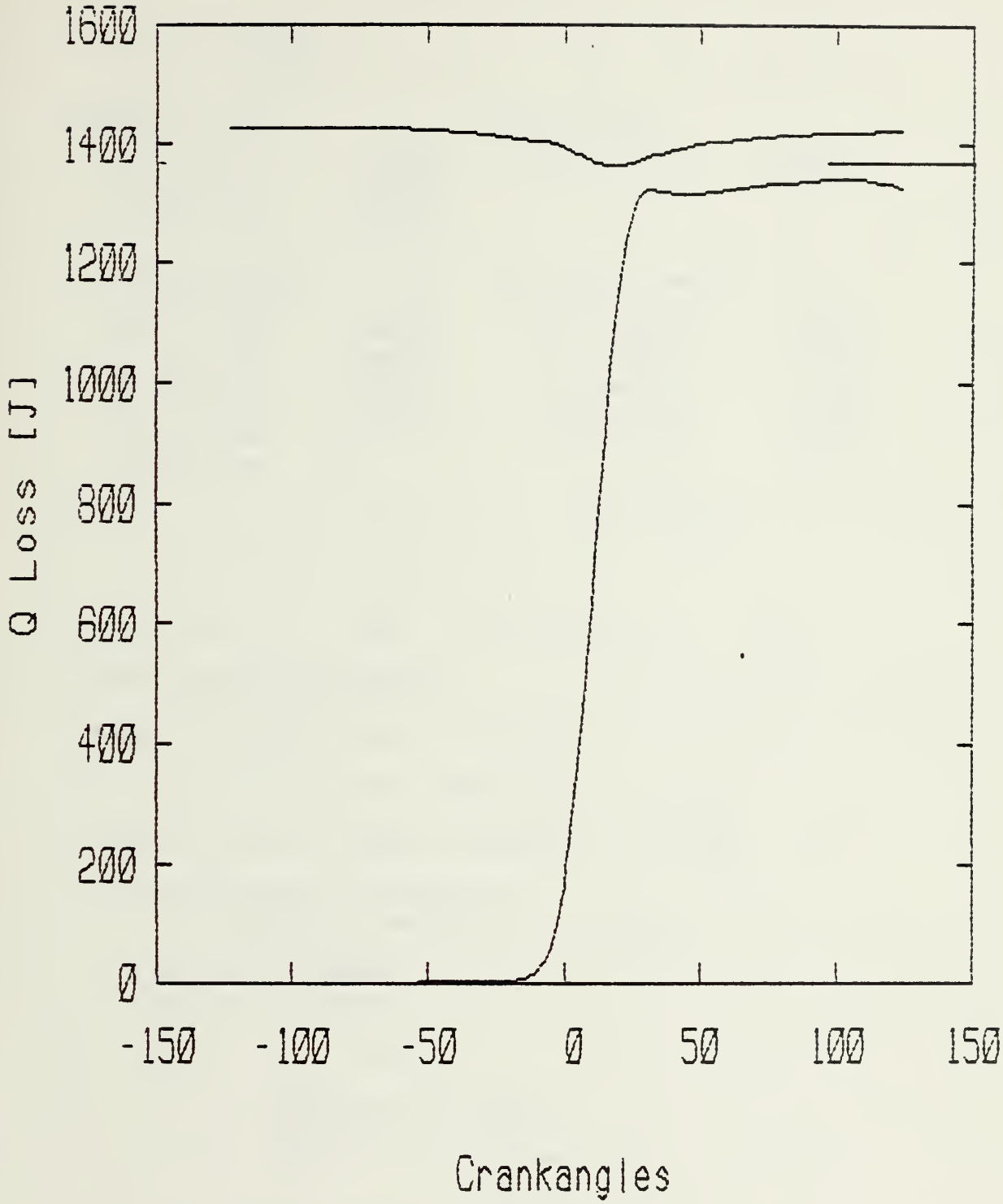

Figure D-4B

1500 RPM WOT

```
Motoring file : RICARD0.40                    43    [a]   1   [b]   43
  Firing file : RICARD0.38                    43    [c]   1   [d]   43

ENGINE RELATED DATA :                  FUEL RELATED DATA :
   [e] Int.Vlv.Cl.=        -124.000        [f]  Fuel Type=       indolene
   [g] Exh.Vlv.Op.=         124.000        [h] LHV [kJ/kg]=       0.431E+05
   [i]  Spark Loc.=         -65.000
   [j] Crev V.[cc]=        0.670E+00

EXPERIMENTAL CONDITIONS :              INPUT VALUES TO ANALYSIS :
   [k] Inl.P.[atm]=           0.350        [l] Area at TDC=          146.600
   [m]        RPM=        2500.000        [n]    Exponent=            0.800
   [o]  Swirl rate=       0.000E+00        [p]   Woshni C1=            2.000
   [q]  Fuel [g/s]=       0.215E+00        [r]   Woshni C2=            0.000
   [s]   Air [g/s]=       0.297E+01        [t] Resid.frac.=           11.200
   [u] Ave. Firing=       Y                [v] Wall tmp[K]=          400.000
   [w] Create Plot=       N

H e a t   R e l e a s e   A n a l y s i s   F o r   RICARDO ENGINE

A N A L Y S I S   F O R   A V E R A G E   C Y C L E

Total Fuel Energy (J) :    444.052     Total Charge at IVC (G) :      0.172

ANALYSIS OF THE RESULTS FOR THIS CYCLE

Maximum pressure: Pmax=13.231 atm   at  15 degrees

Maximum rate of net heat release = 0.124E+02 J/deg   at  10 degrees

Maximum rate of gross heat release = 0.134E+02 J/deg   at  10 degrees

Maximum gross heat release = 0.420E+03 Joules
         i.e:  94.5 % of total energy input,   at 115 degrees

     * 10% of max at -11 degrees
     * 90% of max at  24 degrees

                          THUS:

                  Initiation time =  54 degrees
                  and
                  Propagation time =  35 degrees


Heat transfer at angle of max Qgross = 0.752E+02 Joules
         i.e: 16.9 % of total energy input
```

Figure D-5A

2500 RPM P_I=0.35 atm

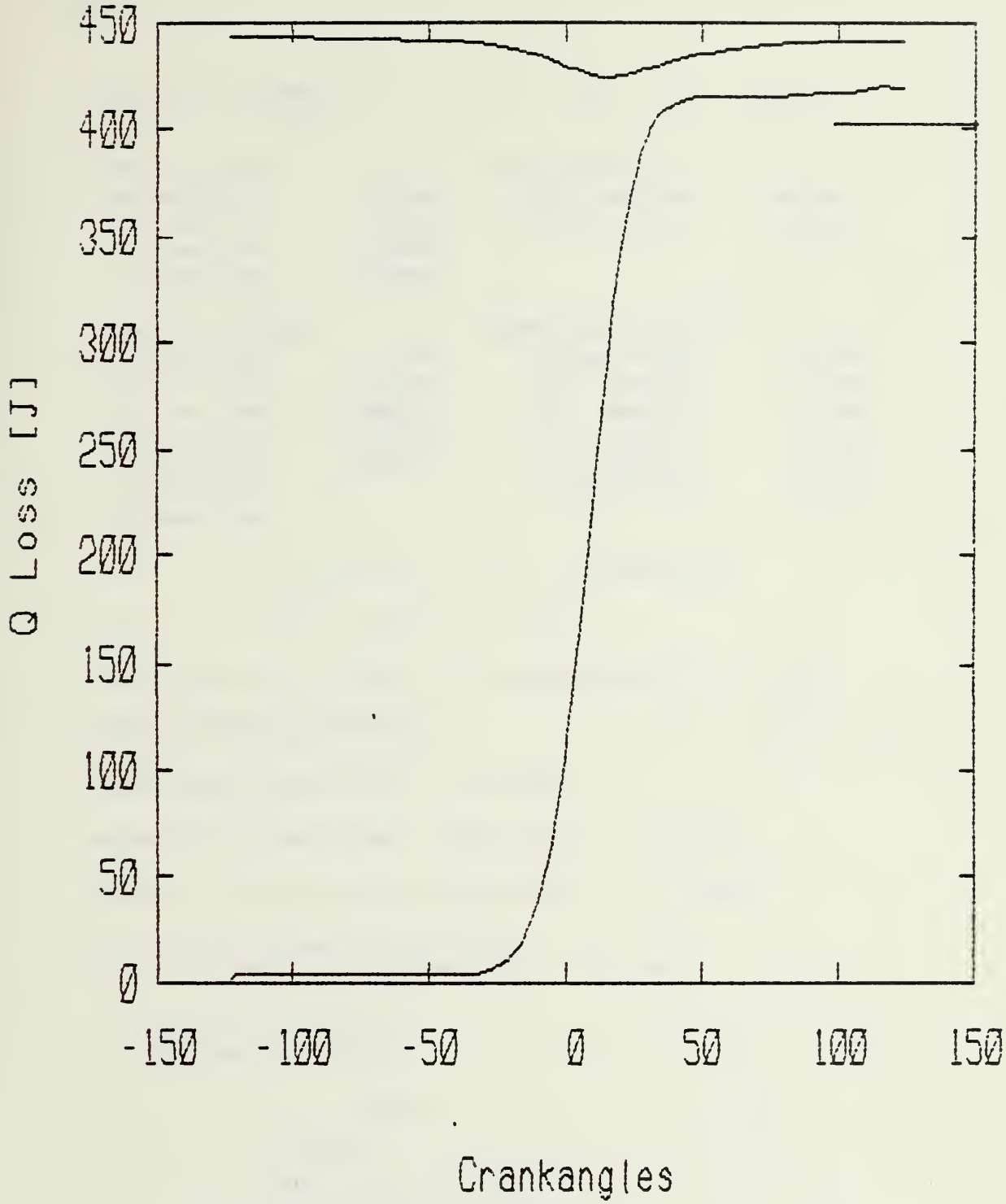

Figure D-5B

2500 RPM P_I= 0.35 atm

```
Motoring file : ricardo.18                    43    [a]  1   [b]  43
  Firing file : ricardo.15                    43    [c]  1   [d]  43

ENGINE RELATED DATA :                  FUEL RELATED DATA :
   [e] Int.Vlv.Cl.=        -124.000        [f]  Fuel Type=       indolene
   [g] Exh.Vlv.Op.=         124.000        [h] LHV [kJ/kg]=       0.431E+05
   [i]  Spark Loc.=         -30.000
   [j] Crev V.[cc]=        0.670E+00

EXPERIMENTAL CONDITIONS :              INPUT VALUES TO ANALYSIS :
   [k] Inl.P.[atm]=           1.003        [l] Area at TDC=          146.600
   [m]         RPM=        2500.000        [n]    Exponent=            0.800
   [o]  Swirl rate=       0.000E+00        [p]   Woshni C1=            2.000
   [q]  Fuel [g/s]=       0.710E+00        [r]   Woshni C2=            0.000
   [s]   Air [g/s]=       0.993E+01        [t] Resid.frac.=            7.000
   [u] Ave. Firing=       y                [v] Wall tmp[K]=          400.000
   [w] Create Plot=       n

H e a t   R e l e a s e   A n a l y s i s   F o r   RICARDO ENGINE

A N A L Y S I S   F O R   A V E R A G E   C Y C L E

Total Fuel Energy (J) :  1469.139     Total Charge at IVC (G) :      0.549

ANALYSIS OF THE RESULTS FOR THIS CYCLE

Maximum pressure: Pmax=42.656 atm   at  18 degrees

Maximum rate of net heat release = 0.574E+02 J/deg   at  11 degrees

Maximum rate of gross heat release = 0.611E+02 J/deg   at  11 degrees

Maximum gross heat release = 0.144E+04 Joules
        i.e:  98.0 % of total energy input,   at  97 degrees

    % 10% of max at  -2 degrees
    % 90% of max at  23 degrees

                          THUS:

                Initiation time =  28 degrees
                and
                Propagation time =  25 degrees


Heat transfer at angle of max Qgross = 0.173E+03 Joules
        i.e: 11.8 % of total energy input
```

Figure D-6A

2500 RPM WOT

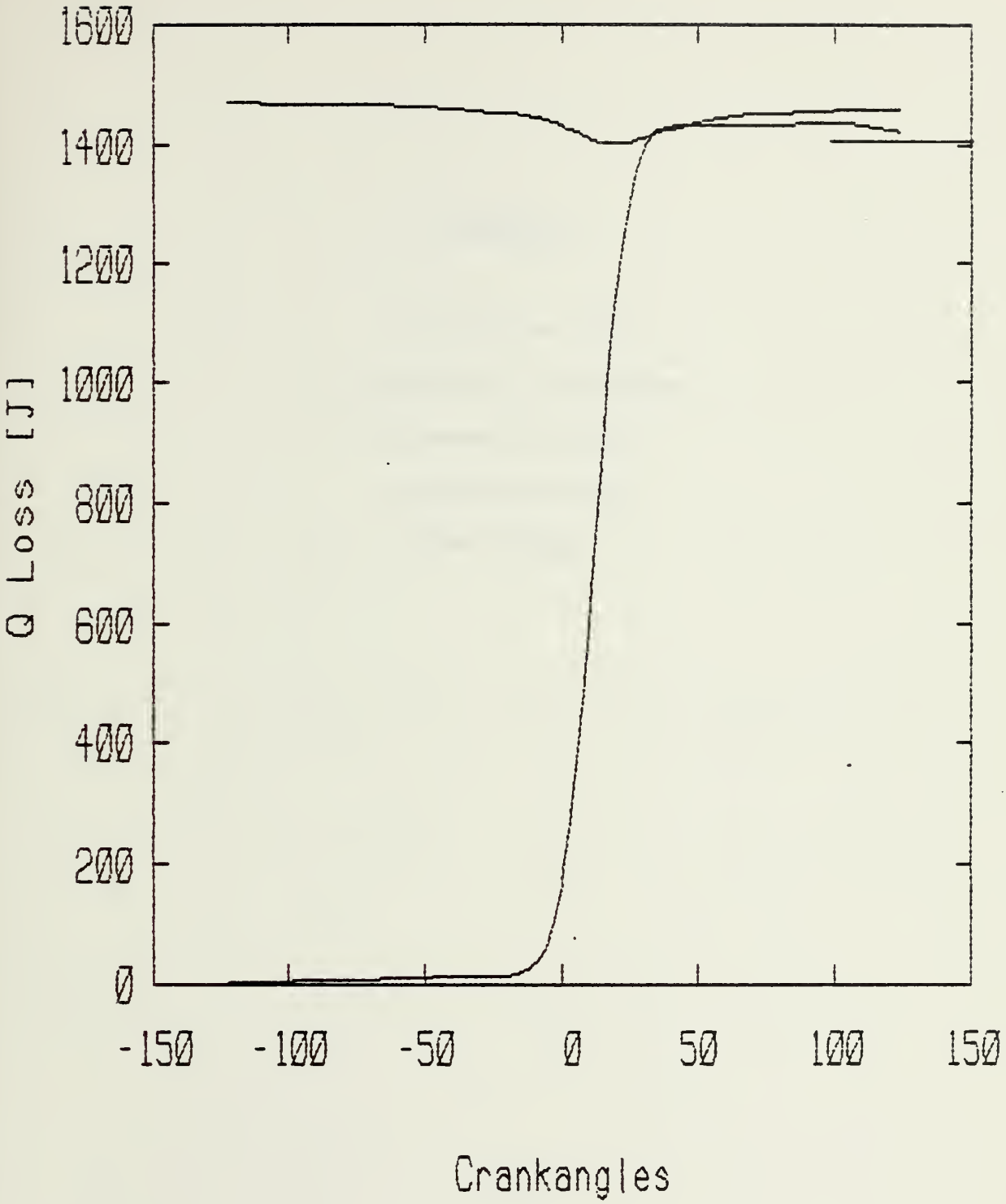

Figure D-6B

2500 RPM WOT

APPENDIX E

Least Squares Error Calculations to Determine the Model Parameters Yeilding "Best Fit" Heat Release

Speed (RPM)	1000	1500	1500	1500	2500	2500	$(\Sigma e^2)^{1/2}$
Intake Pressure (atm)	.36	.35	.44	WOT	.35	WOT	
Chemical Energy Released Mass fuel x LHV x η_{comb}	407	397	520	1368	402	1406	
C_1= 2.0 n = 0.8 V_{CR}= 1.0%							
Q max released (J)	392	411	516	1340	420	1440	
e (J)	15	-14	4	28	-18	-34	52
e_{norm}	0.038	-0.035	0.008	0.021	-0.045	-0.024	0.024
C_1= 2.0 n = 0.8 V_{CR}= 1.5%							
Q max released (J)	394	415	523	1360	424	1460	
e (J)	13	-18	-3	-8	-22	-54	63
e_{norm}	0.032	-0.045	-0.006	-0.006	-0.055	-0.0384	0.087
C_1= 2.5 n = 0.8 V_{CR}= 1.0%							
Q max released (J)	409	431	540	1390	438	1480	
e (J)	-2	-34	-20	-22	-36	-74	93.9
e_{norm}	-0.005	-0.086	-0.039	-0.016	-0.090	-0.053	0.141

Figure E-1

Least squares error fit for the heat release curves

Speed (RPM)	1000	1500	1500	1500	2500	2500	$(\Sigma e^2)^{1/2}$
Intake Pressure (atm)	.36	.35	.44	WOT	.35	WOT	
Chemical Energy Released Mass fuel x LHV x η_{comb}	407	397	520	1368	402	1406	
C_1=2.5 n = 0.8 V_{CR}= 1.5%							
Q max release (J)	412	435	547	1400	442	1500	
e (J)	-5	-38	-27	-32	-40	-94	116.9
e_{norm}	-0.012	-0.096	-0.052	-0.023	-0.100	-0.067	0.164
C_1= 1.0 n = 0.6 V_{CR}= 1.5%							
Q max released (J)	454	468	579	1420	426	1490	
e(J)	-47	-71	-59	-52	-24	-84	144.8
e_{norm}	-0.115	-0.179	-0.113	-0.038	-0.060	-0.060	0.258

$e = [\dot{m}_a$ (g/cyc) x lower heating value(LHV) x η (combustion)] - Q max release (from heat release analysis)

$$e_{norm} = \frac{e}{\dot{m}_a \text{ (g/cyc)} \times \text{LHV} \times \eta \text{ (comb)}}$$

Figure E-1 (continued)

Least squares error fit for the heat release curves

APPENDIX F

GRAPHS FOR COMPARISIONS OF LOADS AND SPEEDS

1) Cylinder Energy

2) Chemical Energy Released

3) Combustion Heat Release Profile

with Model Parameters:

$C_1 = 2.0$

$C_2 = 0.0$

$n = 0.8$

$V_{cr} = 1\ \%$ of V_c

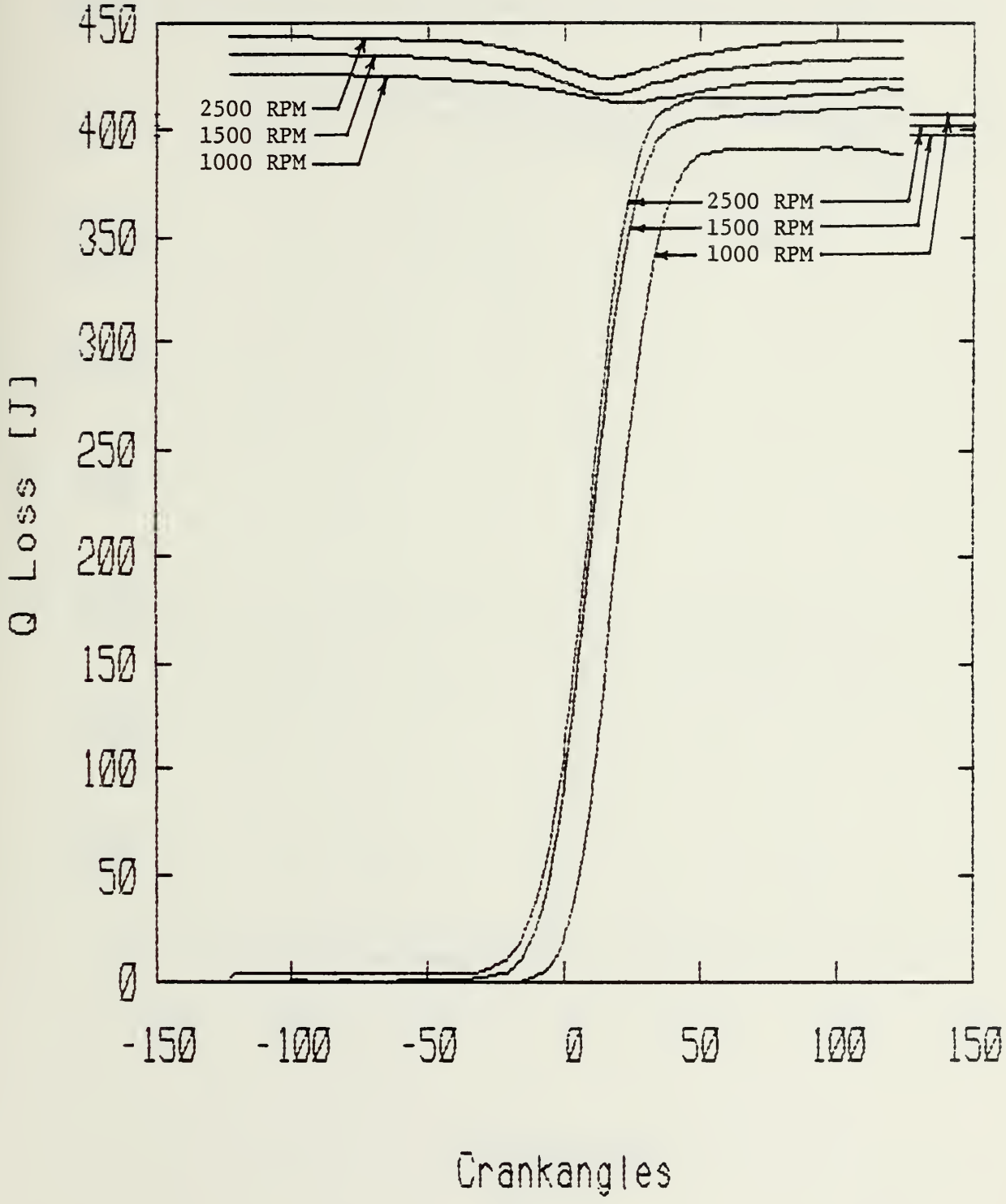

Figure F-1

Comparison of 1000 RPM, 1500 RPM and 2500 RPM at $P_I \simeq 0.35$

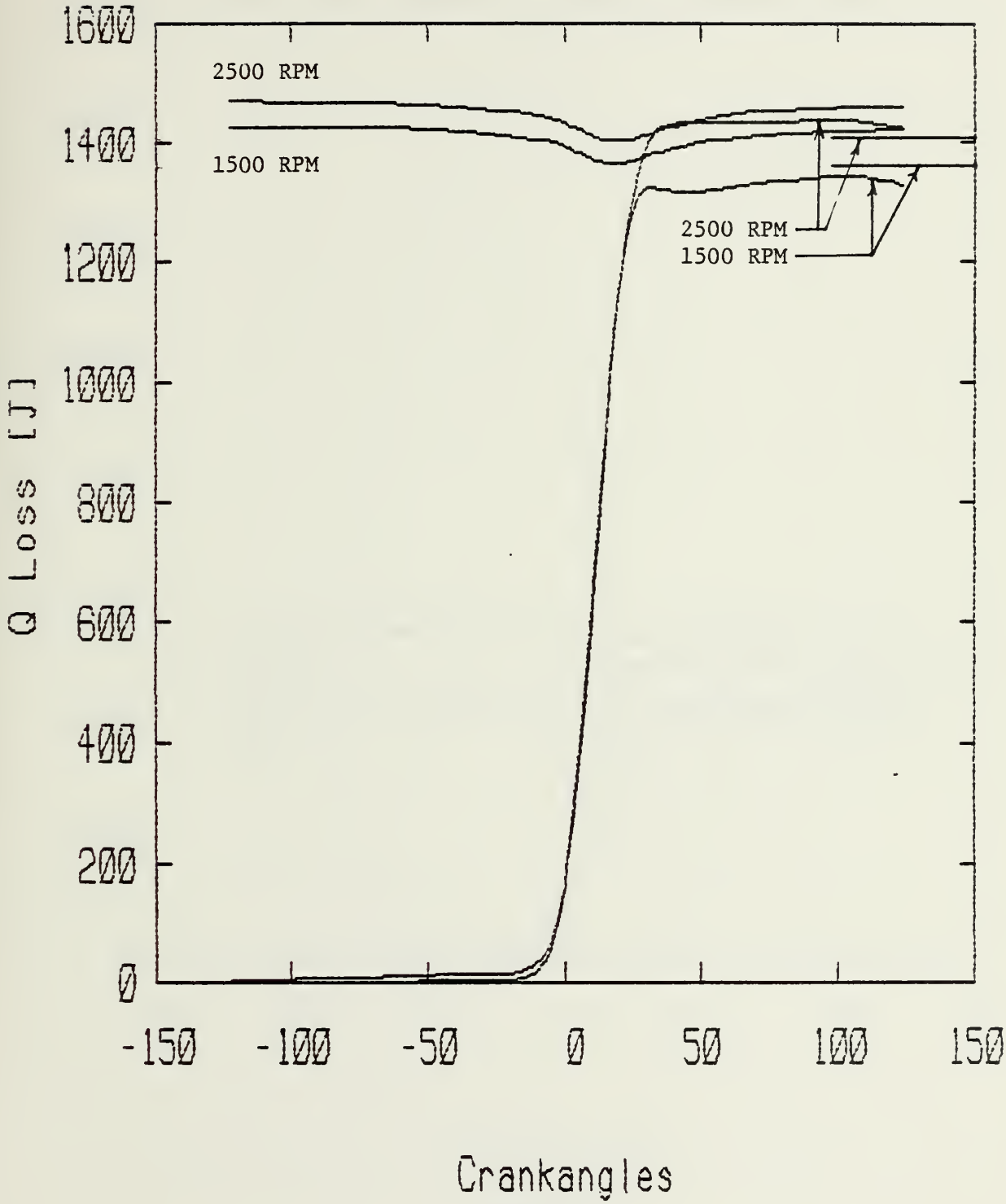

Figure F-2

Comparison of 1500 RPM and 2500 RPM at WOT

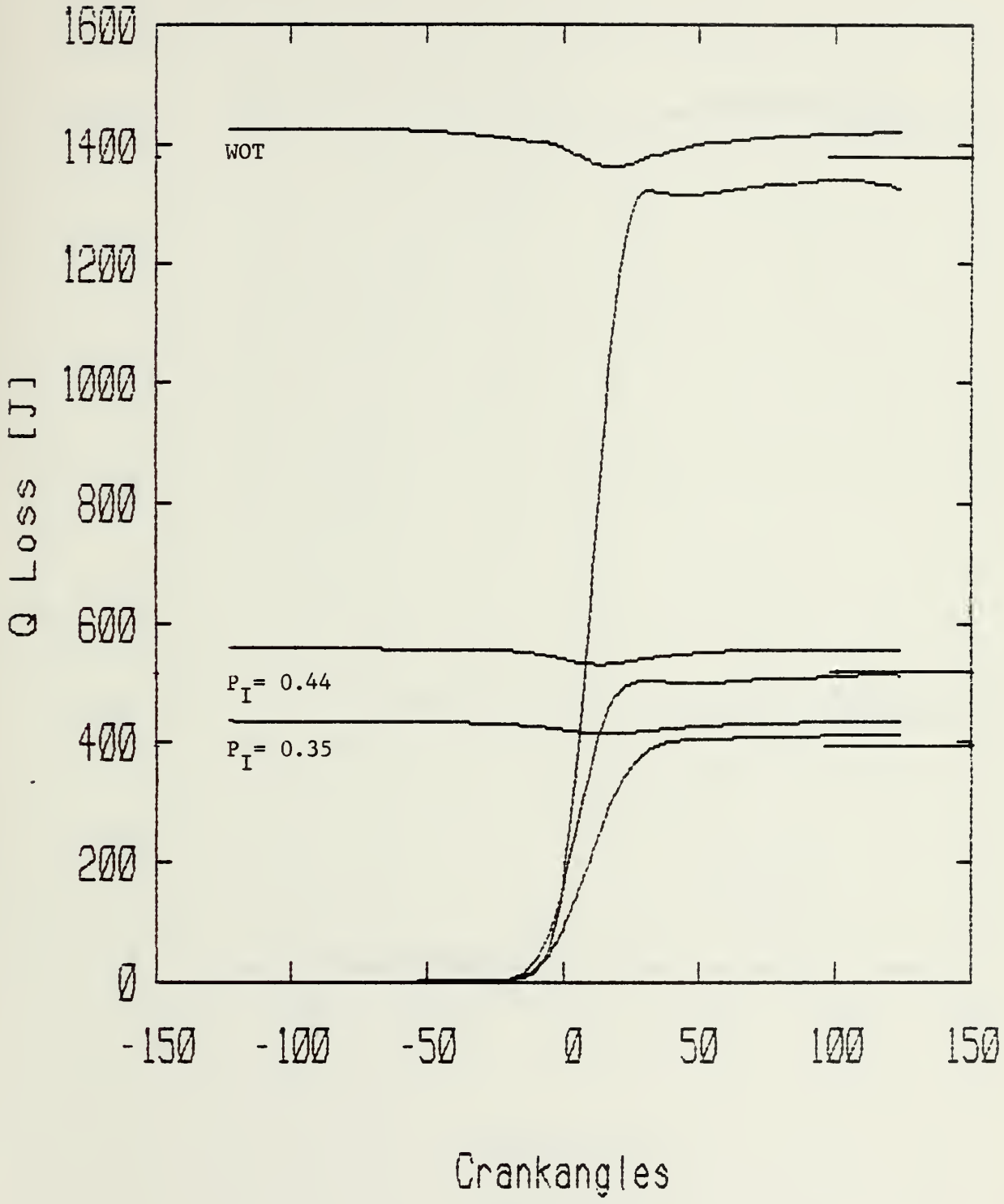

Figure F-3

Comparison of load at 1500 RPM with P_I= 0.35, 0.44, and WOT

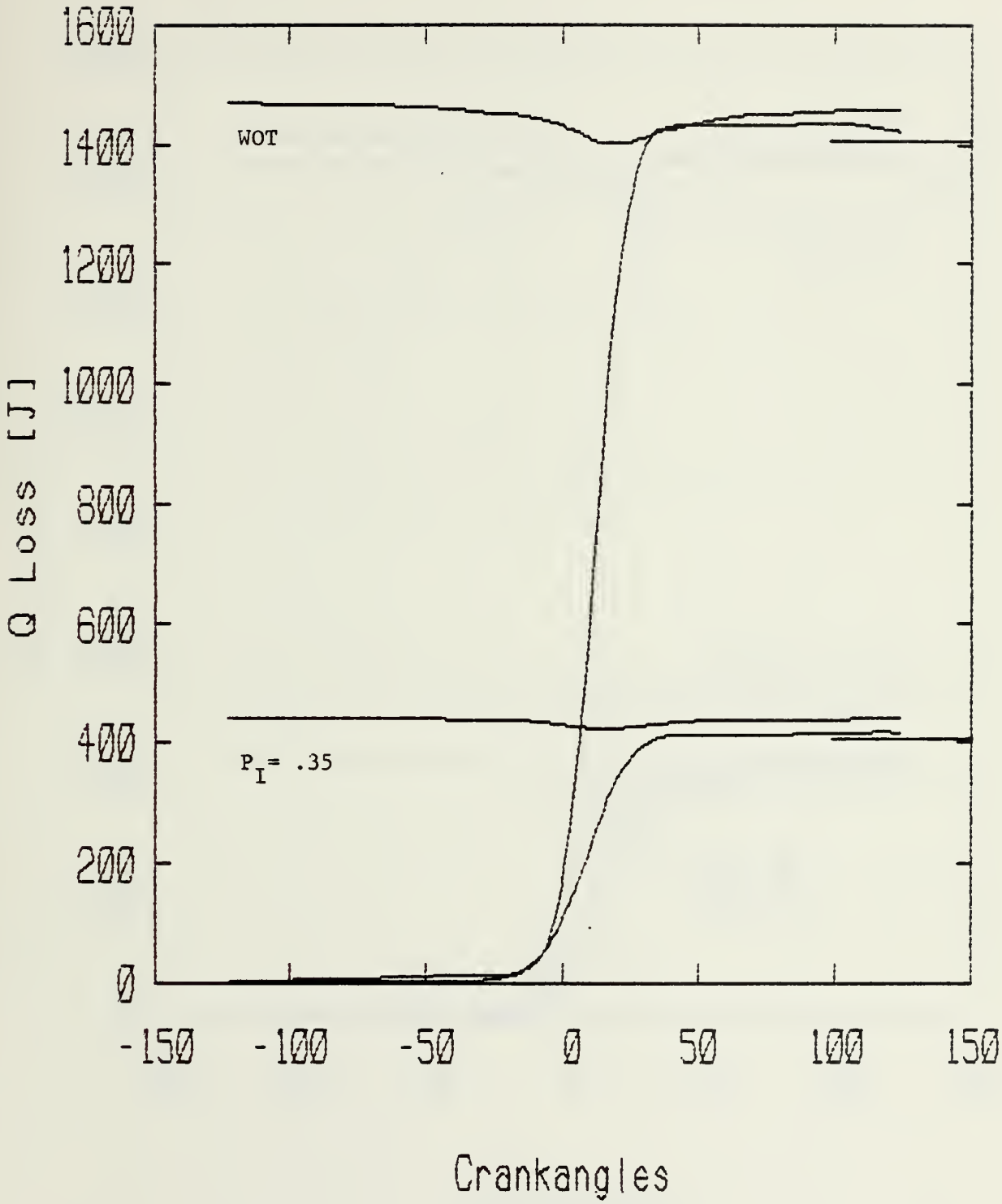

Figure F-4

Comparison of load at 2500 RPM with P_I=.35 and WOT

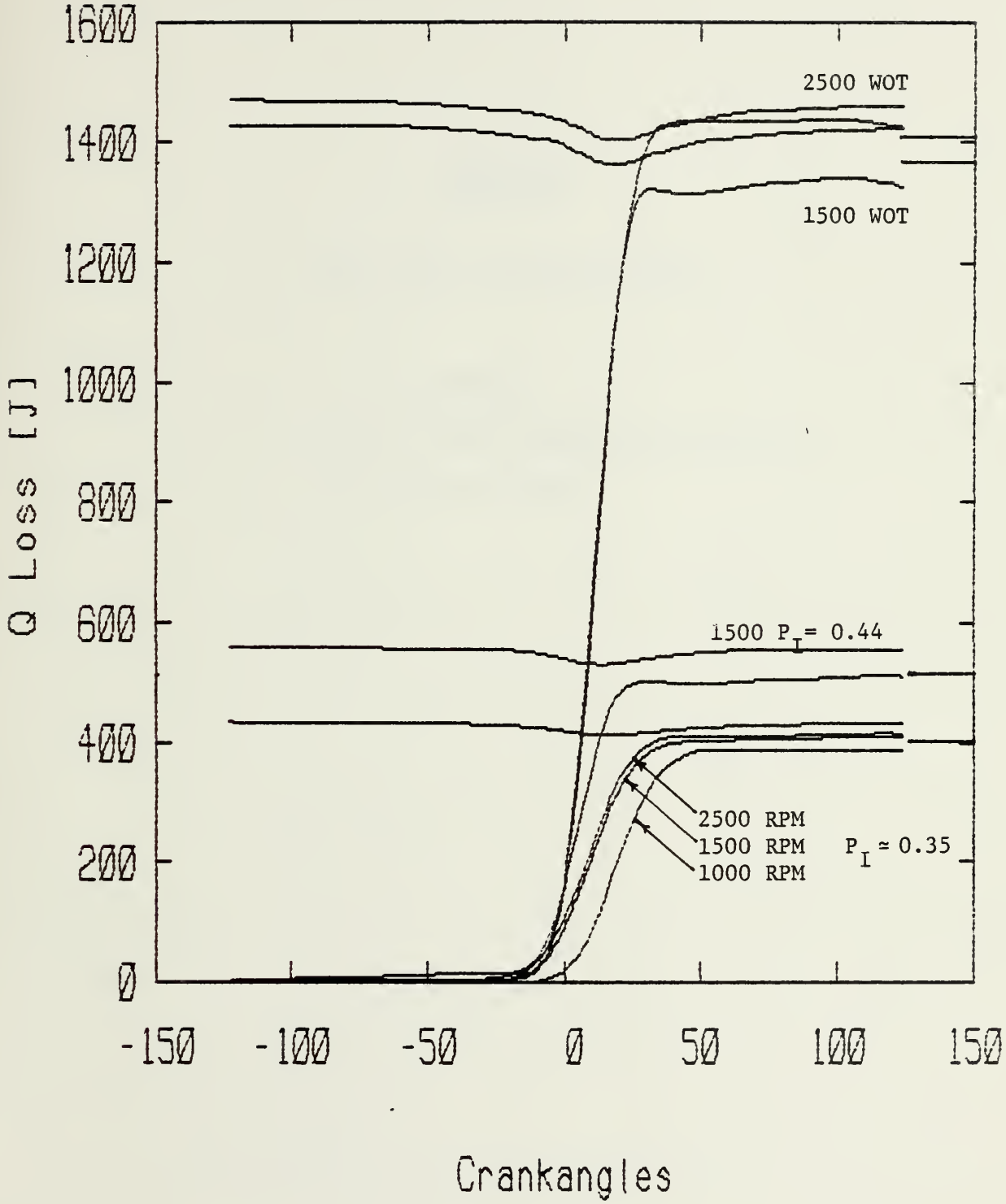

Figure F-5

Profiles of the heat release at the six engine operating points

Appendix G

Fuel - Air Flow Calculations

1. Calculations
2. Air Flow Temperature Corrections
3. Fuel Flow Chart

APPENDIX G

Calculations of Air and Fuel Flow

Air Flow Rate

The scale depends on the maximum position,

(1) For top inclined position = 7.50×10^{-5}

(2) For second position = 3.00×10^{-5}

Air flow (m^3/s) = maximum reading x scale factor x temperature correction (figure G-2)

$$\text{Air flow } \left(\frac{g}{s}\right) = \text{air flow } \left(\frac{m}{s}\right) \times \left(\frac{273}{273 + \text{air intake temp}}\right) \times \left(\frac{P(LFE)}{760}\right) 1.293 \times 10^3$$

where P(LFE) = Barameter reading - pressure drop across the viscous flow meter laminar element

Fuel Flow Rates

$$\text{Fuel Flow } (g/s) = \frac{\text{measured volume flow}(cm^3/min) \times \text{density of Indolene(fig.B-4)}}{60 \times 10^3}$$

Equivalence Ratio Intake

$$\frac{\text{Fuel Flow}(g/s)}{\text{Air Flow g/sec}} \times \frac{1}{14.37} \left(\frac{F}{A}\right) = \text{Equivalence Ratio}$$

VISCOUS FLOW AIR METER

TEMPERATURE CORRECTION FOR METERS CALIBRATED AT 20°C

TEMP DEG C.	VISCOSITY CORRECTION FACTOR	TEMP DEG C.	VISCOSITY CORRECTION FACTOR	TEMP DEG C.	VISCOSITY CORRECTION FACTOR
1	1.052	31	0.972	61	0.903
2	1.049	32	0.969	62	0.900
3	1.047	33	0.967	63	0.898
4	1.044	34	0.964	64	0.896
5	1.041	35	0.962	65	0.894
6	1.038	36	0.959	66	0.892
7	1.035	37	0.957	67	0.890
8	1.033	38	0.955	68	0.888
9	1.030	39	0.952	69	0.886
10	1.027	40	0.950	70	0.884
11	1.024	41	0.947	71	0.882
12	1.022	42	0.945	72	0.880
13	1.019	43	0.943	73	0.878
14	1.016	44	0.940	74	0.876
15	1.013	45	0.938	75	0.874
16	1.011	46	0.936	76	0.872
17	1.008	47	0.933	77	0.870
18	1.005	48	0.931	78	0.868
19	1.003	49	0.929	79	0.866
20	1.000	50	0.927	80	0.864
21	0.997	51	0.924	81	0.863
22	0.995	52	0.922	82	0.861
23	0.992	53	0.920	83	0.859
24	0.990	54	0.918	84	0.857
25	0.987	55	0.915	85	0.855
26	0.984	56	0.913	86	0.853
27	0.982	57	0.911	87	0.851
28	0.979	58	0.909	88	0.850
29	0.977	59	0.907	89	0.848
30	0.974	60	0.905	90	0.847

Figure G-2

Temperature correction chart for air flow calculations

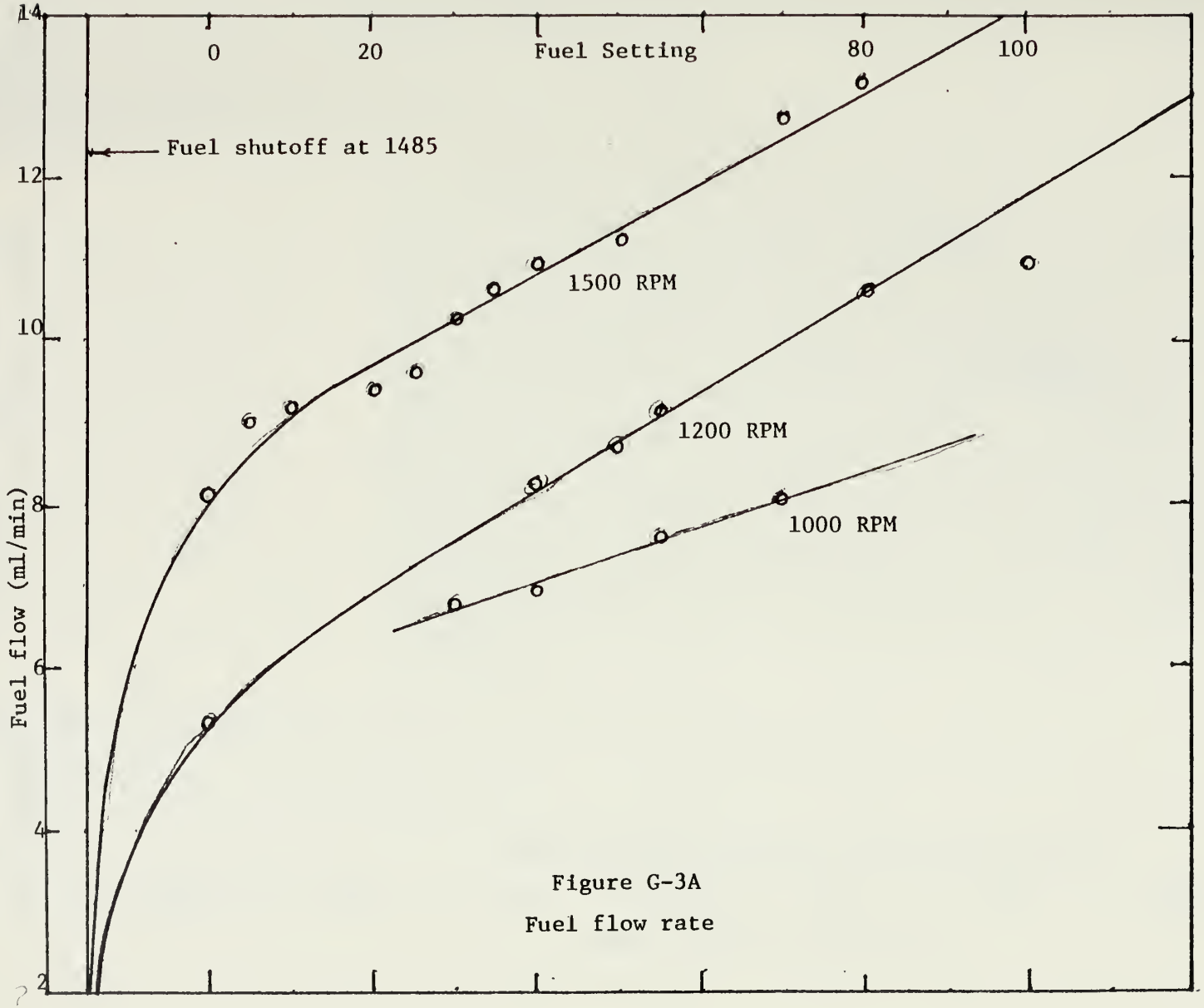

Figure G-3A

Fuel flow rate

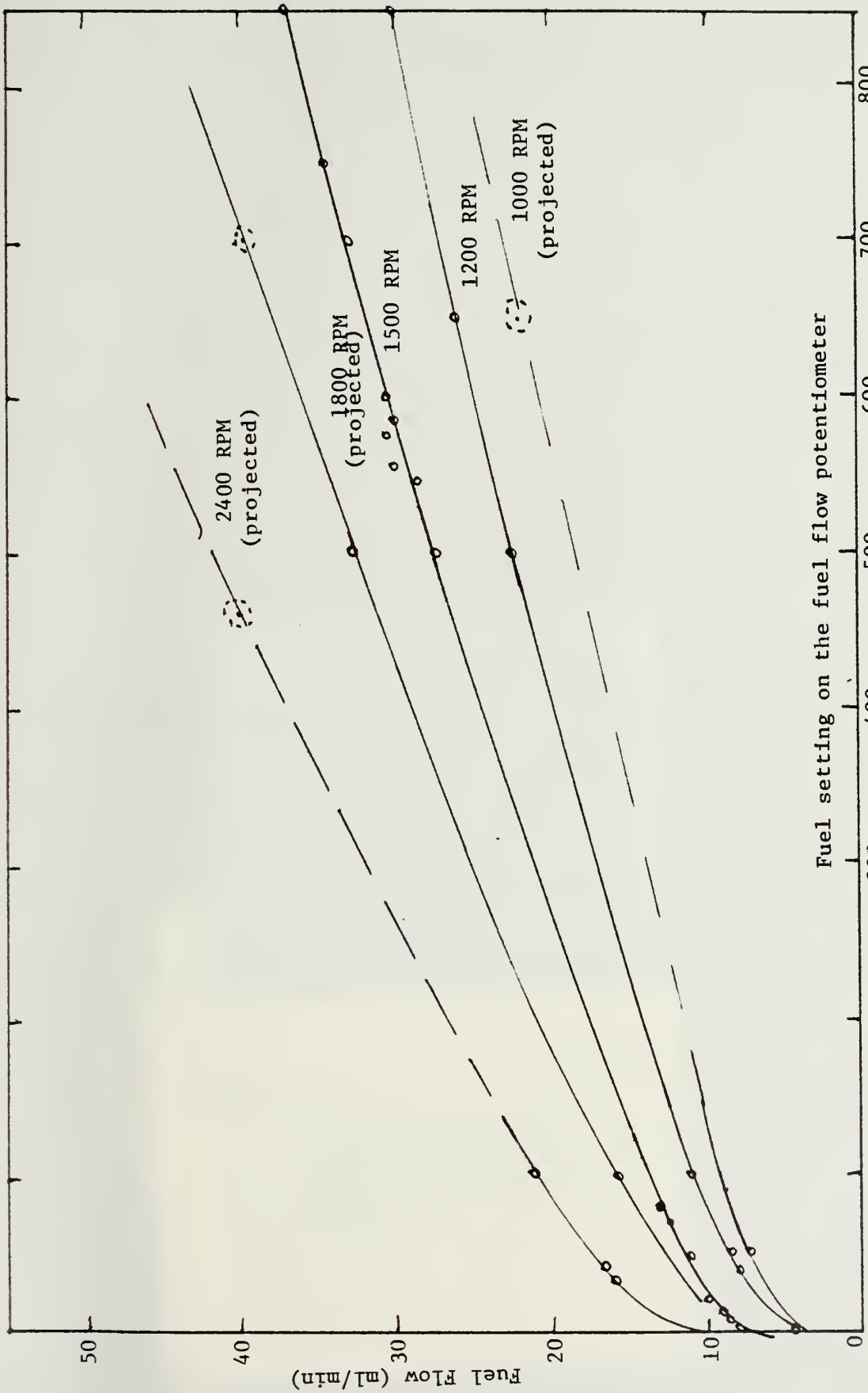

Figure G-3B Fuel Flow Rate

207081

Thesis
N36145 Nelson
Measurement and analysis of spark ignition engine pressure data to determine heat release profiles.

207081

Thesis
N36145 Nelson
Measurement and analysis of spark ignition engine pressure data to determine heat release profiles.

thesN36145
Measurement and analysis of spark igniti
3 2768 002 01806 1
DUDLEY KNOX LIBRARY